

# Dalton Transactions

Accepted Manuscript



This is an *Accepted Manuscript*, which has been through the Royal Society of Chemistry peer review process and has been accepted for publication.

*Accepted Manuscripts* are published online shortly after acceptance, before technical editing, formatting and proof reading. Using this free service, authors can make their results available to the community, in citable form, before we publish the edited article. We will replace this *Accepted Manuscript* with the edited and formatted *Advance Article* as soon as it is available.

You can find more information about *Accepted Manuscripts* in the [Information for Authors](#).

Please note that technical editing may introduce minor changes to the text and/or graphics, which may alter content. The journal's standard [Terms & Conditions](#) and the [Ethical guidelines](#) still apply. In no event shall the Royal Society of Chemistry be held responsible for any errors or omissions in this *Accepted Manuscript* or any consequences arising from the use of any information it contains.

## ***Structural flexibility in crystallized matter : from history to applications.***

G rard F rey<sup> </sup>

<sup> </sup> Acad mie des Sciences & Institut Lavoisier, Universit  de Versailles, 45, Avenue des Etats-Unis, 78035. Versailles Cedex (France)  
e-mail : [gferrey@gmail.com](mailto:gferrey@gmail.com) - [www.gerard-ferrey.org/](http://www.gerard-ferrey.org/)

Structural flexibility corresponds to the dynamic reaction of crystallized solid state matter under the action of an external stimulus<sup>1,2</sup>. This stimulus, which can be either chemicals, temperature, pressure, light, induces atomic movements in the structure which lead, at the molecular level, to significant variations of the cell volume of the solid. The magnitude of these volume changes (corresponding either to an increase or a contraction) can vary in a large range of dimensions, between tenths of   to almost 10 , keeping however the same structural topology (Fig.1).

Fig. 1.- *Scheme of the occurrence of flexibility under the action of an external stimulus.*

This new phenomenon seems intrinsic to porous coordination polymers (PCPs), often labelled as Metal-organic Frameworks (MOFs), a subclass of the well known coordination polymers. This new class of solids, discovered before the nineties<sup>3,4</sup>, corresponds now to several thousands of new structures<sup>5-8</sup>, which make now this domain one of the currently most topical areas in chemistry.

### ***1. Historical aspects.***

The first observation of this phenomenon is due to Kitagawa<sup>9</sup>, who also predicted in the same paper the six possibilities for structures to exhibit flexibility, as a function of the dimensionality of the framework. The second observation, performed independently by two groups interested by hydrated ordered Zr-based alkane mono and diphosphonates, occurred one year later. During dehydration, the linear alkanes act as springs, and they observed an important shrinkage of the structure, which disappears when the solid is rehydrated<sup>10,11</sup>.

In 2002, the third curiosity concerned trivalent metal terephthalates [M<sup>III</sup>(X)[BDC], H<sub>2</sub>O (M = Al<sup>14</sup>, V<sup>12</sup>, Cr<sup>13</sup>, Fe<sup>15</sup>, Ga<sup>16</sup>; X = OH, F), hydrothermally synthesized in my group at 180 C under autogenous pressure. They are now known as the MIL-53 topology (MIL stands for Material of Institut Lavoisier). This structure type oscillates between two configurations corresponding either to large pores (LP) or narrow one (NP). As synthesized, their structure is NP and consists in a three-dimensional network composed of corner-shared trans chains of metallic octahedra (the OH groups being the shared species) linked in the two other directions by terephthalate ions. This determines large unidimensional lozenge-based tunnels within which water molecules are inserted (Fig.2). In terms of nets, the topology of MIL-53 corresponds to a 4<sup>4</sup> lattice. Over the years, this topology has become one of the textbook examples of large reversible flexibility, with thousands of citations<sup>1,2 and refs therein</sup>.

Fig. 2. - *Structures of the closed (left) and open (right) forms of the MIL-53 topology. The insert shows the trans chains of corner sharing octahedra (through OH groups).*

With Al and Cr, the cell volume of their hydrated form NP is close to 1,000  <sup>3</sup>. During their dehydration, it suddenly drastically increases in one step up to ca. 1,500  <sup>3</sup>, while keeping the same topology, but LP. With Fe, the contrary occurs; the cell volume of the anhydrous cell decreases in two steps down to 900 <sup>3</sup> (Fig.3). All these changes are reversible.

Fig. 3.- *The inverse evolution of anhydrous forms of MIL-53(Fe) and MIL-53(Al,Cr), with their changes of space group when the amount of guests progressively increases in the tunnels (acronyms : vnp for very narrow pores, int for intermediary phase, np for narrow pores and lp for large pores).*

For vanadium, during the dehydration,  $V^{3+}$  ions are oxidized into  $V^{4+}$  ions. This implies that the primitive OH groups are replaced by oxide ions within the chains for satisfying the electro-neutrality of the structure. This oxidation creates irreversibility for rehydration ; indeed, after opening of the tunnels during dehydration, the tunnels curiously remain in their large pores (LP) configuration during rehydration. Beyond the fact that, within a same structure type, flexibility depends on the nature of the metallic ion, the vanadium solid (labelled MIL-47) provides an interesting feature. With it, researchers have indeed at their disposal both the flexible and the rigid forms of the same topology. This will be very important when studying on a physical chemistry point of view the roles of host-guest interactions on the flexibility.

## 2. Analysis of the the different parameters influencing the flexibility.

The ca. 50% variation of the cell volumes observed for MIL-53 is not a limit. It can reach, without any decrease of crystallinity, more than 300% during the hydration-dehydration process. The larger magnitude is currently offered by the chromium diphenyl-dicarboxylate MIL-88<sup>17</sup>. In terms of atomic movements, this represents close to 10Å displacements while keeping a perfect crystallinity for the structure.

Fig. 4.- *Scheme of the giant flexibility of MIL-88 (see text). The upper part represents the evolution of the shape and the dimensions of the cage (the trimers appear in green) ; the lower part shows the projection of the extension of the cell (dry for dehydrated solid, As for as-synthesized, Open for the filled cage).*

The current literature describes now many flexible solids. However, beside observation, it is also necessary to physically understand and explain the different reasons of such a phenomenon for, eventually, look later at its eventual applications. These reasons are both structural and energetic. The first require to identify in the structures the potential different degrees of freedom which allow flexibility, both in the inorganic and organic parts of the framework. The energetic reasons concern the guests within the pores and the different interactions (guest-guest and host-guest) that they induce in the structures. Both parameters appear on Fig.5.

Fig. 5.- *The various degrees of freedom in an open structure allowing its flexibility.*

### 2.1. - The structural reasons in the framework

They can be found on three places in the structure : (i) in the inorganic moiety itself ; (ii) in the ligand and its conformation ; (iii) in the junction between the two.

#### 2.1.1. – The inorganic moiety

In the following, it will be labelled 'brick' or 'building block'.

It drastically depends on the conditions of synthesis, particularly temperature and pH. The effect of temperature was nicely illustrated during the search of cobalt(II) succinates<sup>18-21</sup> and the evolution of the number of constituting polyhedra of their bricks, called *nuclearity*. When keeping invariant the other conditions of synthesis, increasing of temperature increases both the nuclearity of the brick and the dimensionality of the inorganic subnetwork. At 60°C, the brick is a single Co octahedron at 60°C ; it becomes a trimer at 100°C, resulting into 1D structures of chains. Above this temperature, the

building block progressively becomes a tetramer, then a pentamer, before exhibiting hexamers at 250°C in a 3D structure. The nuclearity of the building block has also a drastic consequence on the resulting structure. Indeed, the number of possible sites for the attachment of linkers will determine what is called the *connectivity* of the brick (the number of possible bonds with linkers around the brick). This connectivity determines the final structure. It is extremely variable as a function of the nuclearity of the inorganic brick and can now reach more than 20. Fig.6 presents some of the most frequently arrangements with their corresponding connectivity.

Fig. 6.- *Connectivity of some of the most encountered inorganic bricks : four (a), six trigonal pyramid (b), six octahedral c), nine (d,e) and twelve (f). White arrows indicate the different directions toward which the nearest inorganic bricks are found.*

On the other side, pH will play an important role in the coordination of the cation involved in the brick. For instance,  $\text{Al}^{3+}$  cations present a tetrahedral coordination at high pH, and an octahedral one at low pH through a pentagonal one for its intermediary value. This will have an influence on the nuclearity of the resulting building block

For allowing flexibility, a supplementary condition is required for the brick ; the existence of a plane of symmetry. This point will be developed in 2.1.3.

#### 2.1.2. – The linker.

In their central part, the functionalized ligands used in the syntheses can be either rigid (based on phenyl rings or multiple bonds) or present possible changes of the conformation when the carbon chain is aliphatic. Moreover, whatever the nature of the linker (carboxylates (the most commonly used), phosphonates, sulfonates, cyano groups, azolates...), a free rotation between the function and the central part is always allowed and create a degree of freedom. This rotation strongly depends on the steric hindrance of the core of the linker.

#### 2.1.3. – The junction brick-linker.

Their rotations justify the flexibility. The grafting of the functions cited above on the metal of the building block indeed depends on the experimental conditions. According to them, cyanates and azolates are always monotopic, carboxylates can be either di- or monotopic. Phosphonates and sulfonates present three possibilities : mono-, di- and tritopic. In the latter case, they rule out any flexibility while mono- and ditopic cases can generate rotations in the framework, in part responsible of the flexibility (the other part, explained in 2.2, being the host-guest and guest-guest interactions).

These rotations imply coordinated movements between the different parts of the framework. As announced in 2.1.1, the symmetry of the brick will mechanically create or not the possibility for the framework to be flexible. Whatever the nuclearity of the brick, a plane of symmetry is necessary for allowing such cooperative movements. For instance (Fig.7), both the bricks of 'jungle gym' [ $\text{Zn}_2(1,4\text{-BDC})_2(\text{DABCO})$ ], built up of Zn dimers, and MIL-88 ( $\text{Fe}(\text{III})\text{O}$ , ligand) whose building block is a trimer of octahedra, allow these cooperative movements of the carboxylates up and down their plane of symmetry. On the contrary, MOF-5<sup>22</sup>, based on a tetramer of Zn tetrahedra, does not permit these symmetrical displacements and is therefore rigid.

Fig. 7.- *Three examples of bricks allowing or not the possible flexibility of the framework. In the 'jungle gym' [ $\text{Zn}_2(1,4\text{-BDC})_2(\text{DABCO})$ ], based on dimers (a) and in MIL-88 based on a trimer of corner-sharing octahedra*

linked through a  $\mu_3$ -O oxygen (b), the existence of a plane of symmetry in the inorganic brick allows cooperative and symmetrical movements of the ligands attached to the brick (indicated by green arrows). They are not possible for MOF-5 (c), the tetrameric brick of which having no mirror plane.

Once these junctions realized, the topology of the whole framework is created, depending on both the chemical nature, the nuclearity and the connectivity of the inorganic brick, and on the other side, the length and steric hindrance of the linker. They all participate to the eventual flexible character through allowed rotations.

Two examples (Fig.8) illustrate the importance of these rotations/shifts. Fig.8a, devoted to the MIL-53 topology, shows that, depending on the functionalization or not by methyl groups on the phenyl ring, the structure exhibits either its open or closed form, due to the steric hindrance of  $\text{CH}_3$  groups which induce a rotation by ca.  $90^\circ$  of the phenyl ring. The magnitude of this rotation is strongly dependent on the nature of the substituent on this phenyl ring<sup>23</sup>. Fig. 8b concerns the solid  $[\text{Zn}_2(1,4\text{-BDC})_2(\text{DABCO})]$ , (also called 'jungle gym') and the effect of progressive introduction of propane-2,ol (IPA) in the cages of the structure<sup>23-28</sup> which is based on  $\text{Zn}_2$  dimers which, by linkage with four 1,4-BDC molecules, provide 2D square grids. The pillaring of the latter by the nitrogens of DABCO ensures the 3D structure. By a rotation of the COO groups during the introduction, an intermediate structure is observed, which can be described as a shift between layers.

Fig. 8.- Two examples of flexibility due to the influence of diverse types of rotation of the ligands : (a) Pristine MIL-53,  $\text{H}_2\text{O}$  and its grafted homologue with 4 methyl groups on the phenyl ring ; (b) the evolution of the structure of  $[\text{Zn}_2(1,4\text{-BDC})_2(\text{DABCO})]$  during the progressive filling of the cages by propane-2, ol. In the intermediate phase, a shift between two layers is observed due to the rotation of the carboxylate groups of 1,4-BDC (case (a) of Fig.7).

Finally, a topology cannot be flexible when odd cycles of inorganic bricks exist in the network. For example, the 3D vanado-terephthalate MIL-68<sup>29</sup>, a polymorph of MIL-53 with triangular and hexagonal tunnels (6.3.6.3 net) instead of the lozenge one is rigid, due to the presence of non-deformable triangles. It was also proven with the crystallized mesoporous solids MIL-100<sup>30</sup> and MIL-101<sup>31</sup>, which both exhibit pentagonal windows for their cages.

## 2.2. - The energetic reasons of flexibility

They are due to the guests within the pores and the different interactions (guest-guest and host-guest) that they create in the structures. They are of three types :

- the host-host interactions,
- the guest-guest ones
- the host-guest ones

Their relative strengths will play a major role on the flexible character. For showing that, the MIL-53 topology will be mainly used as support.

### a. The host-host interactions.

They are not often encountered. We already mentioned them in the case of the rigid MIL-47. During the oxidation of V(III) into V(IV), the correlative change of the OH groups into oxide ones prevents from the existence of hydrogen bonds between the framework and the guests.

The aluminum 2,6-naphthalene dicarboxylate MIL-69 ( $\text{Al}(\text{OH})$ , *ndc*)<sup>32</sup> provides another example of this type of interaction. At variance to its terephthalate NP homologue MIL-53(Al) which opens during its dehydration<sup>33</sup>, the same experience lets MIL-69 in its narrow pore (NP), due their predominant strong  $\pi$ - $\pi$  intermolecular interactions between two adjacent naphthalene double rings. They block the topology in its NP configuration (Fig.9 right).

If they are weak enough for allowing flexibility in the absence of guests, these interactions depend on temperature through a second order phase transition between the LP and the NP forms. By using neutron thermo-diffraction, Brown *et al*<sup>34</sup> showed that MIL-53(Al),*bdc*, once dehydrated, (Fig.9 left) remains open under N<sub>2</sub> at 300K but, by cooling, it undergoes from 200K a reversible transformation into the NP form. The rehydration of the empty LP form in air at 300K regenerates the initial hydrated NP form. This was confirmed by an independent <sup>129</sup>Xe NMR study of its adsorption isotherms in the range 77-300K<sup>35,36</sup>. The enthalpy of transformation, measured<sup>37</sup> by mercury porosimetry, is close to 5 kJ.mole<sup>-1</sup>. Very recently, a thorough structural study using X-ray diffraction described in detail the evolution of the MIL-53(Al) structure, which is now perfectly known<sup>38</sup>.

Fig. 9.- *Influence of the  $\pi$ - $\pi$  interactions between the ligands on the reversible opening (MIL-53, *bdc*) or not (MIL-53, *ndc*) of the MIL-53 type (*btc* for 1,4-benzene dicarboxylate ; *ndc* for 2,6-naphtalene dicarboxylate).*

b. *The guest-guest and host-guest interactions.*

The guest-guest interactions, in the center of the tunnels, act as a backbone for the other interactions. They depend on the chemical nature of the guests (which are often the molecules of solvent trapped in the cavities of the porous structure). They can have dipolar, quadrupolar (in the case of CO<sub>2</sub>), or Van der Waals origins. The host-guest interactions on their side are essentially related to hydrogen bonding (mainly O...H or N...H). Qualitatively evaluated from the distances considerations, only microcalorimetry is able to quantify them but, despite essential, such measurements are rather rare.

Due to the extreme sensitivity of flexible solids to these interactions, the evolution of the cell volumes is also a qualitative powerful tool for the comparison of their strength. The case of MIL-53(Fe), H<sub>2</sub>O, whose cell volume of the NP form is ca. 900 Å<sup>3</sup>, nicely illustrates that.

When this solid is put in another solvent, the water-new guest exchange is total and immediate, and leads to the LP form at a more or less extent, depending on the nature of the guest. It was interesting to know the intermediate status of the cell between these two extrema. For that, we performed an *in situ* X-Ray diffraction study using the synchrotron radiation at Daresbury at 300K<sup>39</sup> for following the effect of the addition drop by drop of the new solvent, Surprisingly, even for very minute amounts of it, the opening is complete with no intermediary displacements of the Bragg peaks. As soon as the first molecules of the new solvent arrive in contact with the solid, they immediately induce the change of its cell volume by a destruction of the initial interactions. We called '*the forceps effect*' this phenomenon.

Applying this method to many other solvents allowed to establish within the same topology a hierarchy of the strengths of the host-guest interactions. The larger the cell volume in the range 1,000 - 1,500 Å, the weaker the host-guest and guest-guest interactions. This evolution is not dependent on the size of the guest molecules. Only the energies of interaction are concerned. In the whole series, even if the space groups of the structures change, due to small reorientations of the octahedral chains, the topology is preserved. Moreover (Fig. 10), the different cell volumes fit with the theoretical curve representing  $d/D = f(V_{\text{cell}})$ ,  $d$  and  $D$  being the small and long diagonals of the lozenge section of the MIL-53 structure. The third parameter, corresponding to the axis of the chains, remains constant along the evolution.

Fig. 10.- *Left : the effect of an exchange of solvents on the swelling of the MIL-53 topology ; (right) : the evolution of the  $d/D$  ratio (see text) vs. cell volume for some solvents trapped in the tunnels. The black line corresponds the theoretical evolution of  $d/D$  with the volume of the cell. The change of the space groups is also mentioned.*

The length of the small diagonal is also an indicator of the extent of swelling, function of the relative strengths of the guest-guest ( $I_{G-G}$ ) and the host-guest ( $I_{H-G}$ ) interactions. It allows a beginning of

classification of the various openings of the MIL-53 topology (Fig. 11). When  $I_{G-G}$  and  $I_{H-G}$  are strong and of the same order of magnitude, the structure is shrunk (Fig. 11 left). It corresponds to the left part of the curve of Fig. 12. If  $I_{G-G} > I_{H-G}$  (Fig. 11 top right), the strong backbone is preserved but the weakening of the host-guest interactions lead to an opening of the tunnels (medium part of the curve Fig. 12). Finally, when  $I_{G-G} < I_{H-G}$ , the host-guest interactions, despite weak, predominate at such a point that the ordering of the guests in the tunnels disappears. The cell volume becomes maximum (ca.  $1,500 \text{ \AA}^3$ ) and leads to very large pores.

Fig. 11.- *Degrees of opening as a function of the competition between the energies of guest-guest ( $I_{G-G}$ ) and host-guest ( $I_{H-G}$ ) interactions.*

The swelling/shrinkage of the framework also illustrates the onset of confinement effects (equivalent to an internal pressure) which can modify the structural arrangement of guests inside the tunnels. A good example is provided by the comparison of pyridine and lutidine guests within the tunnels of MIL-53 (Fe) (Fig. 12). With lutidine, due to the steric hindrance of the two methyl groups which weakens the O-H...N host-guest interactions, the  $\pi$ - $\pi$  guest-guest interactions between the phenyl rings are favoured and therefore, the ordering of the molecules in the tunnels is similar to that existing in pure solid lutidine with, in both cases, a stacking of the molecules in the LP structure. It is not the case for the inserted pyridine which establishes dominant host-guest interactions in the rather closed form. They oblige the phenyl rings to align, like in lutidine, but this time, the organization of the pyridines is completely different from what happens in the solid pure pyridine, governed by N...H bonds. In other words, the flexibility of MIL-53 induces in this case a phase transition for pyridine, that one can consider as a high pressure form of this solid, due to confinement effects.

Fig. 12.- *Illustration of the confinement effects induced by the flexible MIL-53 structure for pyridine, by comparison to the case of lutidine (see text).*

Once the different reasons of flexibility analyzed, one can come back MIL-53(Al),  $H_2O$  and explain what happens (Fig. 13). The three types of interactions were demonstrated from *in situ* Al, C and H, Xe NMR experiments<sup>33,35,36</sup>: the guest-guest H-O...H-O interactions at the center of the tunnel (green) serve as the backbone and the two kinds of symmetrical host-guest ones: the  $H_{H_2O} \dots O_{\text{carboxylate}}$  (blue) and the  $O_{H_2O} \dots H_{\text{hydroxyl}}$  (purple), joined to the O-O keencap role of the carboxylate ensure the flexibility.

Fig. 13.- *Evidence of the three types of interactions governing the shrinkage of hydrated MIL-53 structure type (guest-guest H-O...H-O (green) at the center of the tunnel;  $H_{H_2O} \dots O_{\text{carboxylate}}$  (blue) and the  $O_{H_2O} \dots H_{\text{hydroxyl}}$  (purple) host-guest ones.*

### 3. Some properties of flexible solids.

Hybrid porous solids (MOFs and PCPs), as other classes of the solid state, exhibit physical properties which could lead in the near future to possible real applications related to the domains of energy, energy savings, environment and health as soon as they evidence both sufficient stabilities toward temperature and humidity, and easy scaling-ups and shapings. For carboxylates, the above stabilities mainly depend on the nature of the metals and on their oxidation number; they generally increase from II to V. Moreover, the extent of these physical properties depends also on the cleverness of chemists who, by pertinent cationic substitutions, can generate properties which did not exist in the as-synthesized solids and which resemble to those of dense solids. The main physical properties of this new class of solids will be briefly recalled before looking at those specific to flexible solids.

### 3.1 - General properties of hybrid porous solids.

For becoming multifunctional materials, MOFs and PCPs must present a large range of properties, far beyond those of adsorption and gas storage, on which a large majority of colleagues focused on. As dense inorganic phases, in the past, obtained a great success in the area of multifunctional materials (superconductors, batteries...), our group decided to look at this aspect for knowing the spectrum of possibilities that MOFs and PCPs could offer in this area, whatever the flexible or rigid character of these phases. Even if it is at the limit of the scope of the present paper, I shall just recall briefly the major properties discovered in the laboratory :

- magnetism<sup>40-43</sup>: most of the 3d transition metal-based MOFs are antiferromagnets, at rather low temperatures, except the Ni-based solids which exhibit ferromagnetism ;
- conductivity<sup>44-47</sup> : MOFs are usually insulating, but the electrochemical introduction of Li metal renders them conductors, combining electronic and ionic conductivity ;
- strong luminescence<sup>48-50</sup> when 4f elements are in the framework, with the first evidence of an 'antenna' effect for MOFs ;
- photoluminescence<sup>51</sup> when Ti<sup>4+</sup>-based MOFs are submitted to UV radiation which provokes a reduction of Ti<sup>4+</sup> into Ti<sup>3+</sup>.
- catalysts<sup>52-54</sup> (this aspect was mainly developed out of the laboratory<sup>54</sup>)
- reversible dehumidifiers<sup>55,56</sup>.

All these studies (and many others), which are just at their very beginning, deserve a deep attention for proving more and more that MOFs and PCPs are among the best multimaterials ever evidenced. For that, clever and creative chemists are already existing !... Indeed, always at the laboratory scale, a new and rich tendency is currently exploding: the technological use of these solids in microstructures through a clever miniaturisation of the processes. These materials currently represent the transition from science to technology. Mainly developed for rigid PCPs, this requires a process optimization (choice of the good material), followed by engineering (a careful control of the geometry of the material and a tuning of the properties for the desired application), and finally an integration into a useful platform (which means the connection with other materials and components). Some results are already striking. Most of them are enumerated in a recent remarkable review by Falcao *et al.*<sup>57</sup>.

### 3.2 - Properties intrinsic to flexible solids.

Their specificity comes from their extreme sensitivity to external stimuli with consequences for the atoms of the internal surface of their frameworks to adapt their proximity, depending on both the steric hindrance of the guests and of the strength of their specific interactions with the surface. This continuous structural adaptation, specific to flexible solids, induces original behaviours, often pioneered in my group, which mainly interest the domain of adsorption/capture/delivery.

The first striking example concerns the comparison of the adsorptions of CO<sub>2</sub> and CH<sub>4</sub> by either the flexible MIL-53(Cr & Al) or its isotopic non-hydroxylated MIL-47(V) at room temperature<sup>58,59</sup>. For MIL-53 type, whereas the CH<sub>4</sub> isotherm exhibits a typical one step type I behaviour, the CO<sub>2</sub> one presents an unexpected hysteretic two-steps shape, hitherto unknown before our experiments (Fig.14a). For CO<sub>2</sub>, the adsorption enthalpy, measured by microcalorimetry, is very exothermic, and lies in the range -45 - -30 kJ.mol<sup>-1</sup>, depending on the adsorbed amount<sup>58</sup>. An original continuous *in situ* powder X-Ray diffraction as a function of the applied pressure<sup>59,60</sup> proved first that, under vacuum, the structure is in its large pores (LP) form. As soon as two CO<sub>2</sub> molecules per tunnel are inserted, the structure suddenly shrinks into its narrow pores form (NP) which remains up to ca. 6bars. This corresponds to the plateau in the isotherm. At higher pressures, the structure reopens and one observes an order-



disorder transition for the CO<sub>2</sub> arrangement. During desorption, the LP form persists down to 2 bars, where NP pores appear, before reopening under vacuum.

The localization of the CO<sub>2</sub> molecules in the tunnel was then possible (Fig. 14b). Their backbone effect along the tunnels is evidenced through CO<sub>2</sub>-CO<sub>2</sub> short distances. The short distances between the oxygen atoms of CO<sub>2</sub> and the hydroxyl groups of the skeleton (< 2Å) indicate that adsorption, in this case, is a physisorption driven by the strong interactions between the quadrupolar CO<sub>2</sub> molecules and the dipolar OH groups. Moreover, a careful IR study<sup>61,62</sup> showed first that the OH groups do not present a significant acid character and that, during adsorption, carbonation of CO<sub>2</sub> does not occur.

Fig. 14.- (a) adsorption isotherms of CO<sub>2</sub> and CH<sub>4</sub> in MIL-53 with, for CO<sub>2</sub> (left), the structural information vs. pressure. For methane, the structure remains in its LP form whatever pressure ; (b) localization of the CO<sub>2</sub> molecules (C: yellow ; O: pink) within the tunnels of the MIL-53 structure. The octahedral chains are in green and the interaction between quadrupolar CO<sub>2</sub> and the OH groups (O : red ; H : white) is visible.

This does not exist with the rigid MIL-47(V). It does not possess OH groups and, consequently, cannot give interactions with CO<sub>2</sub>. The isotherm exhibits the type I shape. The enthalpy of adsorption (-25 - -20 kJ.mol.<sup>-1</sup>) is by far lower than before. The structure remains in its LP form in the whole range of pressure, with disordered CO<sub>2</sub> molecules which progressively fill the tunnels, as evidenced both by the 2D energy maps extracted from Quasi-Elastic Neutron Scattering (QENS) and computer simulations performed by G. Maurin *et al.*<sup>63-68</sup>.

Whatever the structure (MIL-53 or MIL-47), the same disorder of CH<sub>4</sub> guests is observed at 300K. Compared to CO<sub>2</sub>, methane is indeed a spherical apolar molecule which of course cannot give the same type of interactions with the framework. The resulting interactions are not sufficient for generating the flexibility observed with CO<sub>2</sub>. Whatever the amount of methane introduced, MIL-53 remains in its large pore form. The enthalpies of adsorption of methane and of superior alkanes in MIL-53 and MIL-47, measured by microcalorimetry, explained this difference. If the structures are not affected by the introduction of methane, MIL-53 presents the two-steps behavior for superior alkanes. The results<sup>69,70</sup> prove that the enthalpy of adsorption of these species in MIL-53 and MIL-47 is a linear function of the number *n* of carbons of the alkanes with equations of variation of 7.016 + 9.274*n* for MIL-53 and 5.197 + 9.270*n* for MIL-47. This implies that the MIL-53 structure exhibits flexibility only if the enthalpy of adsorption is > ca. 20 kJ.mol.<sup>-1</sup>) which is in agreement with the experimental value observed for CH<sub>4</sub> (-17 kJ.mol.<sup>-1</sup>).

This thorough study, completed by the NMR study of the adsorption of xenon on MIL-53(AI)<sup>35,36</sup>, further allowed numerous computer simulations in front of experimental data (Figs. 15&16). They concerned first the simulation by Maurin *et al.* of the shape of the curve (Fig. 15a) and the hysteretic structural modifications (Figs. 15b,c) as a function of temperature and pressure<sup>71,72 and refs therein</sup>, a study which also predicted the temporal variations of the MIL-53 cell volume as a function of the number of CO<sub>2</sub> molecules introduced in the tunnels (Fig. 15d,e). This also shows that the adsorption, in all the cases, is extremely fast (< 350 ps).

Fig. 15.- (a) Current simulation (red) vs. experience (black) of the two-steps behavior; (b) Simulation of the second order hysteretic LP-NP phase transition vs. temperature ; (c) Simulation of the second order hysteretic LP-NP phase transition vs. pressure; (d,e) variation with time of the MIL-53 cell volume as a function of the number of CO<sub>2</sub> molecules introduced in the tunnel.

On the other side, developing a new approach by DFT calculations, Boutin, Coudert and Fuchs<sup>73-75</sup> were able to establish the T,P phase diagram of MIL-53 when CO<sub>2</sub>, CH<sub>4</sub> or Xe fill the tunnels (Fig. 16).

Fig. 16.- The (T,P) phase diagram of the LP-NP transition for three types of molecules inserted : CO<sub>2</sub>, CH<sub>4</sub> and Xenon (with courtesy of A. Boutin, F.-X. Coudert and A. Fuchs).

From 2008, MIL-53 and MIL-47 were often used as model structures for studying the dynamics of some guests within their tunnels as a function of the presence of OH groups (MIL-53) or not (MIL-47) in the framework. For that, experimental data coming from Quasi-Elastic Neutron Scattering (QENS) were combined with molecular dynamics simulations. The gases involved were CO<sub>2</sub><sup>76,77</sup> and CH<sub>4</sub><sup>78</sup> alone or in mixture<sup>79</sup>, alkanes<sup>69,80-83</sup>, aromatics<sup>84-88</sup>, water<sup>89-91</sup> and H<sub>2</sub><sup>92-94</sup>.

For the two first gases, it was shown that their transport diffusivities are larger than those of zeolites. In the case of MIL-53 filled with CO<sub>2</sub><sup>76</sup>, an increase from the NP to LP is observed, while keeping a 1D microscopic diffusion mechanism, evidenced from 2D free energy maps. For methane in MIL-53<sup>78</sup>, despite a similar but less pronounced 1D diffusion mechanism, the diffusion process is slower than in MIL-47 with respective times of residence of 5.4 and 3.3 ps.

When light alkanes (ethane to butane) in LP MIL-47 are concerned<sup>80</sup>, the rotation of ethane is isotropic whereas that of butane is better reproduced as an uniaxial rotational model. The situation is intermediate with propane. These alkanes do not exhibit any strong interaction with the  $\mu_2$ -O of the skeleton. The 2D free energy maps also indicate a 1D microscopic diffusion mechanism. Surprisingly, the self-diffusion coefficients decrease from ethane to butane. This experimental trend evokes a « blowgun » effect, n-butane behaving like a dart flying in a tube. For higher alkanes (C9-C16)<sup>81</sup>, the experimental diffusivities are about one order of magnitude higher than in the zeolite silicalite. The lower activation energies for diffusion indicate less conformational changes in this 1D-channel type MOF, compared to zeolite. When MIL53 is the host<sup>82</sup>, the shape of the isotherms depends on the number of carbons in the alkane. For C3 and C4, which exhibit a two-steps behaviour, modelization of the isotherm requires the analytical 'phase mixture' procedure of Maurin<sup>83</sup> for predicting the fractions of both NP and LP forms in the transition zone.

The adsorption of some aromatics (benzene, xylene) in these two solids was also studied. Benzene molecules inserted in MIL-47 move in a corkscrew motion<sup>86</sup>, as already observed with bacteria and during RNA polymerase translocation. Also, the insertion of xylene in MIL-53 at different loadings, followed by H<sup>2</sup> NMR, has a controlled influence on the rotation dynamics of the phenylene rings of the terephthalate<sup>87</sup>. This dynamics is very sensitive to the loading of xylene guests in MIL-53. The rotation rate is higher and the activation barrier lower for the LP state for the poorly loaded material. The two latter have inverse variations at high loadings. When the rigid MIL-47 is used<sup>88</sup>, experience and simulations agree for all the xylene isomers to show an unusual non-monotonous evolution of self-diffusivity coefficient with temperature. At low temperature, the xylene molecules are close to the internal surface, with a high activation energy barrier. In the high temperature regime, the xylenes are located at the center of the tunnels and the activation energy for the diffusion is lower.

The simulation of the historical case of water in MIL-53 is recent<sup>89-91</sup> and used different approaches. Salles *et al.*<sup>89</sup> were the first to look at this aspect. They considered the water molecule as a rigid body, and used Newtonian dynamics of the water and the framework. Later, Paesani<sup>90</sup> took into account quantum dynamical effects. In 2013, Coudert and Boutin<sup>91</sup> refined the results by means of DFT-based molecular dynamics simulations. They all agree to explain the hydrophilic character of the NP form and the mildly hydrophobic one for the LP structure. From QENS experiments and 2D free energy maps, it appears that, in NP, the 1D diffusion mechanism for water is strongly confined in the middle of the pores and that the diffusion continues along the direction of the tunnels, whereas a jump sequence is preferred for LP, the  $\mu_2$ -OH groups acting as steric barriers. Moreover, Coudert and Boutin<sup>91</sup> paid attention to the behavior of the OH groups and to the water molecules bound to  $\mu_2$ -OH and their dynamics.

For the first, while its oxygen atom is rather constrained and has a low amplitude of movement (0.2Å), the position of the H atom (and therefore the orientation of the  $\mu_2$ -OH groups) varies more widely

around the Cr-O-Cr plane in both the NP and the LP forms. The wagging of  $\mu_2$ -OH is harmonic. When water molecules are considered in the NP form, they rotate rather freely while keeping intact the hydroxyl-water hydrogen bond. During this rotational diffusion, it appears from the calculations that the water's H atom sometimes comes in close vicinity to the oxygen of a carboxylate of the skeleton, even for short times of residence. This confirms the previous experimental results of our group, extracted from NMR studies<sup>14,33</sup>. The situation is different when water is inserted at high loadings. The molecules are highly disordered, with a large distribution of  $O_{\mu_2\text{-OH}} - O_{\text{water}}$  distances and the organization of water molecules in the LP form is close to the behavior of 'bulk' water with however some differences.

Finally, with  $\text{H}_2$ , stored in large amounts at 77K (3.7wt.% for MIL-53) with hysteresis<sup>92</sup>, a very high  $\text{H}_2$  diffusion is observed from QENS experiments<sup>93,94</sup>. At low loadings, the diffusivity of hydrogen is about two orders of magnitude higher than in zeolites. Such a high mobility was never experimentally observed before. Even at high loadings, the fits of QENS spectra show a 1D diffusion model for  $\text{H}_2$  in MIL-53 with jumps of ca. 7(1) Å close to the distance between two consecutive  $\mu_2$ -OH groups (6.8Å). A 3D behaviour is observed with MIL-47.

All these calculations, applied to various guests, opens a promising direction to improve the selectivity of MOFs by playing both on the sensitivity of flexible MILs to adapt their aperture to various guests and on their selective energies of interaction with the framework.

For example, whereas the adsorption of  $\text{CO}_2$  and  $\text{CH}_4$  in empty MIL-53 was described in detail (see above), a preferential  $\text{CO}_2$  adsorption is observed when a mixture of the gases is sent on this solid<sup>95</sup>. The phenomenon is completely different when taking the NP MIL-53,  $\text{H}_2\text{O}$  instead of MIL-53 as adsorber<sup>96</sup>. Up to ca. 10 bars (Fig. 17a), a 'gate effect' is observed with almost no adsorption of these two gases. Above, only  $\text{CO}_2$  is adsorbed, not  $\text{CH}_4$ .

This selectivity of MIL-47 was tested by De Vos *et al.* for the different xylene isomers and ethylbenzene<sup>97</sup>. The different positions they occupy in the tunnels indicate different host-guest interactions (Fig. 17b). Therefore, using MIL-47 as a chromatographic separator, they proved that the separation performed on an equal mixture of them leads to a quantitative separation within 20mn at room temperature.

Fig. 17.- a) *The drastic difference of behavior between MIL-53 and MIL-53,H<sub>2</sub>O used as adsorbers for CO<sub>2</sub> and CH<sub>4</sub>.* (b) *The quantitative separation of xylene isomers using MIL-47 as separator.* (L. Alaerts, C. E. A. Kirschhock, M. Maes, M. A. van der Veen, V. Finsy, A. Depla, J. A. Martens, G. V. Baron, P. A. Jacobs, J. F. M. Denayer and D. E. De Vos, *Selective Adsorption and Separation of Xylene Isomers and Ethylbenzene with the Microporous Vanadium(IV) Terephthalate MIL-47*, *Angew. Chem., Int. Ed.*, 2007, 46, 4293–4297. Copyright Wiley-VCH Verlag GmbH & Co. KGaA. Reproduced with permission.)

The last property that I shall mention illustrates the ability of the flexible solid to establish tight and energetical contacts with the guest. It is particularly true for the storage and delivery of drugs. Initially discovered for rigid MOFs in 2006 in our group<sup>98</sup>, this property also applies to flexible solids<sup>99-100</sup>. This makes MOFs the best drug nano-vectors discovered up to now<sup>101</sup>, far better than the liposomes currently used. They combine excellent stability in physiological media, storage of important amounts of drugs and long times deliveries. For example, the MIL-53 structures, not only adsorb large quantities of Ibuprofen (1g/g of solid), but deliver the latter quantitatively in a quasi-linear manner (Fig. 18). Delivery is complete after the unprecedented time of 3 weeks. Due to their non-toxicity and their sensitivity in medical imaging, the Fe-based solids are chosen for *in vitro* and *in vivo* characterizations. Beside the test drug Ibuprofen, the MIL-53 structure adsorbs and delivers many other drugs with different hydrophilic/hydrophobic characteristics (Busulfan against leukemia, doxorubicin against breast and kidney cancers, AZT-TP against HIV...) and also poisonous gases ( $\text{CO}_2$ ,  $\text{H}_2\text{S}$ ) which, at high doses are lethal but, at small doses, are very useful in heart surgery<sup>102</sup>. The

time of delivery strongly depends on the nature of the drug. For the flexible Fe-based MOFs, it occurs in the range 2-11 days.

Fig. 18.- *Delivery of ibuprofene as a function of time for MIL-53(Cr) and -(Fe).*

#### 4. The onset of industrial applications of flexible solids.

Indeed, there is a gap between interesting properties evidenced at the laboratory scale, which could *potentially* find applications in several domains, and real applications at the industrial scale. Indeed, global trends that influence our civilization and economy are essential. A growing world population, an increasing demand on energy and climate protection implies important innovations in the domains of energy, energy savings, environment and health. Due to their properties, detailed above, MOFs and PCPs can, in the future, play a major role in these domains.

To reach such an objective, this implies, before any production, the upstream verification of some criteria :

- the non-toxicity of the chosen solids ;
- the reliability and the high yield of their syntheses ;
- the test of their various stabilities (temperature, humidity, chemistry) at the laboratory scale ;
- the low cost of the precursors and solvents employed in the reactions ;
- their ability to scale-up from the gram to 100g at least, through the verification of the invariance of the properties for increasing amounts of solid ;
- their easy shaping (nanoparticles, thin films...) for dedicated applications (health, sensors...).

Among the thousands of hybrid porous solids discovered up to now, only a few satisfy these six conditions. It is the merit of the company BASF to have applied these criteria, far before others, to the development of some MOFs and PCPs through international patents<sup>103-106</sup>. Among the solids they produce under the label BASOLITE (MOF-5, HKUST-1, MILs...), and through a nice collaboration between us, a particular attention was paid to our aluminum-based solids.

For economical reasons, they currently represent the best compromise between costs, yields and stability<sup>107 and refs therein</sup>. The flexible MIL-53 was the first to be produced industrially (BASOLITE A100) but, undoubtedly, the best material is currently the rigid Al fumarate with the MIL-53 topology. It cumulated a room temperature synthesis in water, using Al sulfate as precursor, interesting surface area (> 1,300 m<sup>2</sup>/g), short times of reaction, excellent yields (98%) and an outstanding Space-Time-Yield ratio (> 3,600 kg/m<sup>3</sup>/day). It is now commercialized (Fig. 19) at the industrial scale (BASOLITE A520). Its considerable methane storage capacity at room temperature makes that BASF now produces a system storing natural gas for heavy duty vehicles. A prototype of the latter was launched in February 2013 at Ludwigshafen (Fig.19). If methane is stored at 35 bars, the autonomy of the vehicle is ca. 350 km. This allows to think about the use of A520 for the exploitation and the transport of gas shales.

Fig. 19. – (a) *The launch of the BASF prototype equipped with the system of methane storage for vehicles, (b) The pilot plant for the production of A520 ; (c) bulk A520 ; (d) Pills based on MIL-53 (A100) [b, c & d with courtesy of BASF] ; (e) nanoparticles of MIL-53(Fe)<sup>82</sup> ; (f) thin films of optical quality<sup>109-114</sup>.*

However, and for the same reasons, projects are in progress, focusing PCPs for purification of air and water<sup>100,103</sup>. BASF develops also now the use of flexible MOFs for adsorption of odors and hazardous

volatile products contained in air. Moreover, we have shown that our Al-based products can perfectly reversibly adsorb hydrogen sulfide<sup>77, 102</sup>, which could be used for the purification of natural gas from H<sub>2</sub>S for a potential substitution to amine treatments.

Finally, all these above properties and applications of flexible solids prove that this class of solids is already very rich, but also consider that flexibility is a bistable system between the NP and the LP forms. However, it was recently shown by J.R. Long and us<sup>115</sup> that the concept of flexibility is much more general than bistability. Indeed, a new cobalt(II) pyrazolate presents five steps in the flexible behavior instead of two. They were structurally characterized; this opens the way for more sophisticated applications, particularly in separation processes.

\* \* \* \* \*

**Acknowledgements :** *The author is very grateful toward all those who participated to this adventure either in the laboratory (C. Serre, T. Loiseau, C.Mellot, F. Millange, N.Guillou, C. Livage, F. Taulelle, M. Haouas and all their PhD students) or outside. I am particularly indebted to the groups of G. Maurin (Montpellier), P. LLewellyn (Marseille), H. Jobic (Lyon), M. Daturi (Caen), G. De Weireld (Louvain) and of J.-S. Chang (Taejon, South Korea) for their unvaluable long-time contributions. Special thanks are also addressed to the local scientists of the Large Instruments Facilities of ILL Grenoble and of Soleil in Orsay (E. Suard, I. Margiolaki, Y. Fiinchuk). Finally, I appreciated very much the excellent industrial collaboration I had with U. Müller and his group of BASF in Ludwigschaften (Germany).*

## References

- S. Horike, S. Shimomura, S. Kitagawa, *Nature Chem.*, 2009, **1**, 695
- C. Serre, G. Férey, *Chem. Soc. Rev.* 2009, **38**, 191
- Y. Saito, T. Higuchi, *Bull. Soc. Chim. Japan* 1959, **32**, 1221.
- B. F. Hoskins, R. Robson, *J. Am. Chem. Soc.* 1989, **111**, 5962.
- G. Férey, *Chem. Soc. Rev.* 2008, **37**, 191.
- Themed issue on Metal-organic frameworks, *Chem. Soc. Rev.* 2009, **38**, 201-518.
- Themed issue on Hybrid Materials, *Chem. Soc. Rev.* 2011, **40**, 453-1162.
- Themed issue : Metal-Organic Frameworks, *Chem. Rev.* 2012, **112**, 673-1268.
- S. Kitagawa, M. Kondo, *Bull. Soc. Chim. Japan* 1998, **71**, 1739
- G. Alberti, M. Murcia-Mascaros, R. Vivani, *J. Am. Chem. Soc.* 1998, **120**, 9291
- A. Clearfield, *Prog. Inorg. Chem.* 1998, **47**, 373.
- K. Barthelet, J. Marrot, D. Riou, G. Férey, *Angew. Chemie Int. Ed. Engl.* 2002, **41**, 281.
- C. Serre, F. Millange, C. Thouvenot, M. Nogués, G. Marsolier, D. Louër, G. Férey, *J. Am. Chem. Soc.* 2002, **124**, 13519.
- T. Loiseau, C. Serre, C. Huguénard, G. Fink, F. Taulelle, M. Henry, M., T. Bataille, G. Férey, *Chem. Eur. J.* 2004, **10**, 1373.
- F. Millange, N. Guillou, R.I. Walton, J.-M. Grenèche, I. Margiolaki, G. Férey, *Chem. Comm.* 2008, 4732-4734.
- C. Volkringer, T. Loiseau, N. Guillou, G. Férey, E. Elkaim, A. Vimont, *Dalton Trans.* 2009, 2241.
- C. Serre, C. Mellot-Draznieks, S. Surblé, N. Audebrand, Y. Filinchuk, G. Férey, *Science*, 2007, **315**, 1828.
- C. Livage, C. Egger, M. Nogués, G. Férey, *J. Mater. Chem.* 1998, **8**, 2743.
- C. Livage, C. Egger, G. Férey, *Chem. Mater.* 1999, **11**, 1546.
- C. Livage, C. Egger, G. Férey, *Chem. Mater.* 2001, **13**, 410.
- P. M. Forster, A.R. Burbank, C. Livage, G. Férey, A.K. Cheetham, *Chem. Comm.* 2004, 368.
- H. LI, M. Eddaoudi, M. O'Keeffe, O.M. Yaghi, *Nature* 1999, **402**, 276.
- T. Devic, C. Serre, G. Maurin, G. Férey, *J. Mater. Chem.* 2012, **22**, 10266.
- K. Seki, W. Mori, *J. Phys. Chem. B*, 2002, **106**, 1380.
- D.N. Dybtsev, H. Chun, K. Kim, *Angew. Chemie Int. Ed. Engl.* 2004, **43**, 5033.
- H. Chun, D.N. Dybtsev, H. Kim, K. Kim, *Chem. Eur. J.* 2005, **11**, 3521.
- S. Horike, R. Matsuda, D. Tanaka, S. Matsubara, M. Mizuno, K. Endo, S. Kitagawa, *Angew. Chemie Int. Ed. Engl.* 2006, **45**, 7226.
- K. Uemura, Y. Yamasaki, Y. Komagawa, K. Tanaka, H. Kita, *Angew. Chemie Int. Ed. Engl.* 2007, **46**, 6662
- K. Barthelet, J. Marrot, D. Riou, G. Férey, *Chem. Comm.* 2004, 520.
- G. Férey, C. Serre, C. Mellot-Draznieks *et al.*, *Angew. Chem. Int. Ed.* 2004, **43**, 6296.
- G. Férey, C. Mellot-Draznieks, C. Serre *et al.*, *Science*. 2005, **309**, 2040.
- T. Loiseau, C. Mellot-Draznieks, M. Haouas, F. Taulelle, G. Férey, *Comptes-rendus Chimie*. 2004, **8**, 765.
- T. Loiseau, C. Serre, M. Haouas, F. Taulelle, G. Férey, *Chemistry, Eur. J.* 2004, **10**, 1373.
- C.M. Brown *et al.*, *J. Am. Chem. Soc.* 2008, **130**, 11813.
- M.-A. Springuel-Huet, A. Gédéon, G. Férey *et al.*, *Angew. Chem. Int. Ed.* 2009, **48**, 8314.
- M.-A. Springuel-Huet, A. Gédéon, T. Loiesau, G. Férey *et al.*, *J. Am. Chem. Soc.* 2010, **132**, 11599.
- R. Denoyel, A. Fuchs, A. Boutin, G. Férey *et al.*, *Angew. Chem. Int. Ed.* 2010, **49**, 7526,
- C. Nanthamathée, S.L. Ling, B. Slater, M.P. Attfield, *Chem. Mater.* 2015, **27**, 85.
- G. Férey, C. Serre *et al.* *Chem. Soc. Rev.* 2011, **40**, 550.
- M. Cavellé, C. Livage, G. Férey *et al.* *Solid State Sciences*, 2002, **4**, 267.
- N. Guillou, S. Pastre, C. Livage, G. Férey, *Chem. Comm.* 2002, 2358.
- N. Guillou, C. Livage, M. Nogués, G. Férey *Angew. Chem. Int. Ed.* 2003, **42**, 644.
- N. Guillou, C. Livage, M. Drillon, G. Férey *Angew. Chem. Int. Ed.* 2003, **42**, 5314.
- G. Férey, M. Morcrette, C. Serre, M.L. Doublet, J.-M. Grenèche, J.-M. Tarascon, *Angew. Chem. Int. Ed.* 2007, **46**, 3259.
- G. De Combarieu, M. Morcrette, I. Margiolaki, G. Férey, J.-M. Tarascon, *Chem. Mater.* 2009, **21**, 1602.
- G. De Combarieu, M. Morcrette, I. Margiolaki, G. Férey, J.-M. Tarascon, *Electrochem. Comm.* 2009, **11**, 1881.
- A. Fateeva, C. Serre, J.-M. Grenèche, M. Morcrette, J.-M. Tarascon, G. Férey, *Eur. J. Inorg. Chem.* 2010, **24**, 3780.
- C. Serre, F. Pelle, G. Férey *et al.* *J. Mater. Chem.* 2004, **14**, 1540.
- F. Pelle, S. Surblé, C. Serre, G. Férey, *J. Luminescence*. 2007, **122-123**, 492.
- F. Pelle, S. Surblé, C. Serre, G. Férey, *J. Solid State Chem.* 2010, **183**, 795.
- C. Serre, T. Frot, L. Rozes, C. Sanchéz, G. Férey, *J. Am. Chem. Soc.*, 2009, **131**, 10857.
- J.-S. Chang, M. Daturi, C. Serre, G. Férey *et al.* *Angew. Chem. Int. Ed.* 2008, **47**, 4144.
- D.-Y. Hong, C. Serre, G. Férey, J.-S. Chang *et al.* *Adv. Funct. Mater.* 2009, **19**, 1537.
- D. Farrusseng, S. Aguado, C. Pinel, *Adv. Funct. Mater.* 2009, **19**, 1537.
- Y.-K. Seo, J.-S. Chang, M. Daturi, P. Llewellyn, C. Serre, G. Férey, *Adv. Mater.* 2012, **24**, 806
- H. Furukawa *et al.* *J. Am. Chem. Soc.*, 2014, **136**, 4369.
- P. Falcao, R. Ricco, C.M. Doherty, K. Liang, A.J. Hill, M.J. Styles, *Chem. Soc. Rev.* 2014, **43**, 5513.
- S. Bourrelly, P. Llewellyn, C. Serre *et al.* *J. Am. Chem. Soc.*, 2005, **127**, 13519.
- P. Llewellyn, G. Maurin, G. Férey *et al.* *J. Am. Chem. Soc.*, 2009, **131**, 13002
- C. Serre, P. Barnes, G. Férey *et al.*, *Adv. Mater.*, 2007, **19**, 2246.
- A. Vimont, M. Daturi, G. Férey *et al.* *Chem. Comm.* 2007, **31**, 3291.
- S. Bourrelly, M. Daturi, C. Serre, G. Férey *et al.* *J. Am. Chem. Soc.*, 2010, **132**, 11599.
- G. Maurin *et al.* *Phys. Chem. Chem. Phys.* 2010, **12**, 12478.
- N. Rosenbach, G. Maurin, H. Jobic *et al.* *Angew. Chem. Int. Ed.* 2008, **47**, 6611.
- A. Ghoufi, G. Maurin, G. Férey *et al.* *Angew. Chem. Int. Ed.* 2008, **47**, 8487.
- N. Rosenbach, G. Maurin, H. Jobic *et al.* *Angew. Chem. Int. Ed.* 2009, **48**, 8335.
- D. Kolokolov, H. Jobic, G. Maurin, G. Férey *et al.*, *Angew. Chem. Int. Ed.* 2010, **49**, 4791.
- D. Kolokolov, H. Jobic, G. Maurin, G. Férey *et al.*, *J. Phys. Chem.* 2012, **28**, 15093.
- I. Deroche, P. Trens, F. Fajula, G. Férey *et al.*, *J. Phys. Chem. C* 2011, **115**, 13868.
- N.A. Ramsahye, P. Trens, F. Fajula, P. Llewellyn, G. Maurin *et al.*, *J. Phys. Chem. C* 2011, **115**, 18683.
- I. Beurroies, M. Boulhout, P. Llewellyn, G. Férey, C. Serre, R. Denoyel, *Angew. Chem. Int. Ed.* 2010, **49**, 7526.
- A. Ghoufi, C. Zhong, G. Maurin, G. Férey, *J. Phys. Chem. C* 2012, **116**, 13289.
- A. Boutin, M.-A. Springuel-Huet, G. Férey, F.-X. Coudert, A. Fuchs, *Angew. Chem. Int. Ed.* 2009, **48**, 8314.
- A. Boutin, F.-X. Coudert, M.-A. Springuel-Huet, G. Férey, A. Fuchs, *J. Phys. Chem. C* 2010, **114**, 22237.

75. F.-X. Coudert, *Chem. Mater.* 2015, **27**, 1905.
76. F. Salles, H. Jobic, A. Ghoufi, *et al. Angew. Chem. Int. Ed.* 2009, **48**, 8335.
77. F. Salles, H. Jobic, T. Devic, G. Maurin *et al.*, *ACS Nano* 2010, **4**, 143.
78. N. Rosenbach, H. Jobic, F. Salles, G. Maurin, *et al.*, *Angew. Chem. Int. Ed.* 2008, **47**, 6611.
79. F. Salles, H. Jobic, D.I. Kolokolov, G. Maurin *et al.*, *J. Phys. Chem. C*, 2013, **117**, 11275.
80. H. Jobic, N. Rosenbach Jr., A. Ghoufi, D.L. Kolokolov, G. Maurin *et al.*, *Chemistry Eur. J.*, 2010, **16**, 10337.
81. S. Rives, H. Jobic, F. Ragon, T. Devic, C. Serre, G. Férey, J. Ollivier, G. Maurin. *Mic. Mes. Mater.* 2012, **164**, 259.
82. N. Rosenbach, A. Ghoufi, G. Férey, G. Maurin, *Phys. Chem. Chem. Phys.* 2010, **12**, 6428.
83. A. Ghoufi, G. Maurin, *J. Phys. Chem. C*, 2010, **114**, 6496.
84. D.L. Kolokolov, H. Jobic, A.G. Stepanov *et al. Angew. Chem. Int. Ed.* 2010, **49**, 4791.
85. D.L. Kolokolov, H. Jobic, A.G. Stepanov *et al. Eur. Phys. J.* 2010, **189**, 263
86. D.L. Kolokolov, H. Jobic, A.G. Stepanov *et al. J. Phys. Chem C.* 2012, **116**, 15093.
87. D.L. Kolokolov, A.G. Stepanov, H. Jobic, *J. Phys. Chem C.* 2014, **118**, 15978.
88. S. Rives, D.L. Kolokolov, H. Jobic, A.G. Stepanov, G. Maurin *et al. J. Phys. Chem C.* 2013, **117**, 6293.
89. F. Salles, S. Bourrelly, H. Jobic, C. Serre, G. Férey, G. Maurin *et al. J. Phys. Chem C.* 2011, **115**, 10764.
90. J. Cirera, J.C. Sung, P.B. Howland, F. Paesani, *J. Chem Phys.* 2012, **137**, 054704.
91. V. Haigis, F.-X. Coudert, R. Vuilleumier, A. Boutin, *Phys. Chem. Chem. Phys.* 2013, **15**, 19049.
92. G. Férey, M. Latroche, C. Serre *et al. Chem. Comm.* 2003, 2976.
93. F. Salles, H. Jobic, G. Maurin, G. Férey *et al., Phys. Rev. Lett.* 2008, **100**, 245901
94. F. Salles, D.I. Kolokolov, H. Jobic, G. Maurin, G. Férey *et al.*, *J. Phys. Chem. C*, 2009, **113**, 7802.
95. L. Hamon, P. LLewellyn, G. Maurin, G. Férey *et al. J. Am. Chem. Soc.*, 2009, **131**, 17490
96. S. Bourrelly, P. LLewellyn, G. Férey *et al. J. Am. Chem. Soc.*, 2005, **127**, 13519.
97. D.E. De Vos *et al. Angew. Chem. Int. Ed.* 2007, **46**, 4293.
98. P. Horcajada, C. Serre, G. Férey *et al. Angew. Chem. Int. Ed.* 2006, **45**, 5974.
99. P. Horcajada, C. Serre, G. Férey *et al. J. Am. Chem. Soc.*, 2008, **130**, 13519.
100. P. Horcajada, C. Serre, G. Férey, P. Couvreur, R. Gref *et al. Nature Mater.*, 2010, **9**, 172
101. P. Horcajada, G. Maurin, R.E. Morris, P. Couvreur, C. Serre *et al., Chem. Rev.*, 2012, **112**, 1232 and refs. therein.
102. A.C. McKinley, R. Morris, P. Horcajada, C. Serre, G. Férey, *Angew. Chem. Int. Ed.* 2010, **49**, 6260.
103. U.Müller, M.Schubert, M. Hesse, H. Pütter, H. Wessel, J. Huff, M. Guzman, WO2006/122920.
104. U.Müller, M. Hesse, H. Pütter, M.Schubert, M. Guzman, J. Huff, WO2006/125739
105. M. Schubert, U.Müller, H. Mattenheimer, M. Tonigold, WO2007,023119.
106. C. Kiehner, U.Müller, M.Schubert, F. Teich, WO2008/122542.
107. U. Müller *et al., Chem. Soc. Rev.* 2009, **38**, 1284.
108. M. Graab, N. TRukhan, S. Maurer, R. Gummaraju, U. Müller, *Mic. Mes.Mater.* 2012, **157**, 131.
109. A. Demessence, C. Serre, C. Boissière, D. Grosso, C. Sanchez, G. Férey, *Chem. Comm.* 2009, 7149.
110. A. Demessence, C. Serre, C. Boissière, D. Grosso, C. Sanchez, G. Férey, *J. Mater Chem.* 2010, **20**, 7676.
111. A. G. Marquez, C. Serre, G. Férey, C. Boissière, D. Grosso, C. Sanchez, *Eur. J. Inorg. Chem.* 2012, **32**, 5165.
112. J. Gascon, F. Kapteijn, *Angew. Chem. Int. Ed.* 2010, **49**, 1530.
113. D. Zacher, O. Shekkah, C. Wöll, R. Fischer, *Chem. Soc. Rev.* 2009, **38**, 1418.
114. O. Shekkah, J. Liu, R. Fischer, C. Wöll, *Chem. Soc. Rev.* 2011, **40**, 1081.
115. F. Salles, G. Maurin, C. Serre, P. LLewellyn, J.R. Long, G. Férey, *J. Am. Chem. Soc.*, 2010, **132**, 13782.

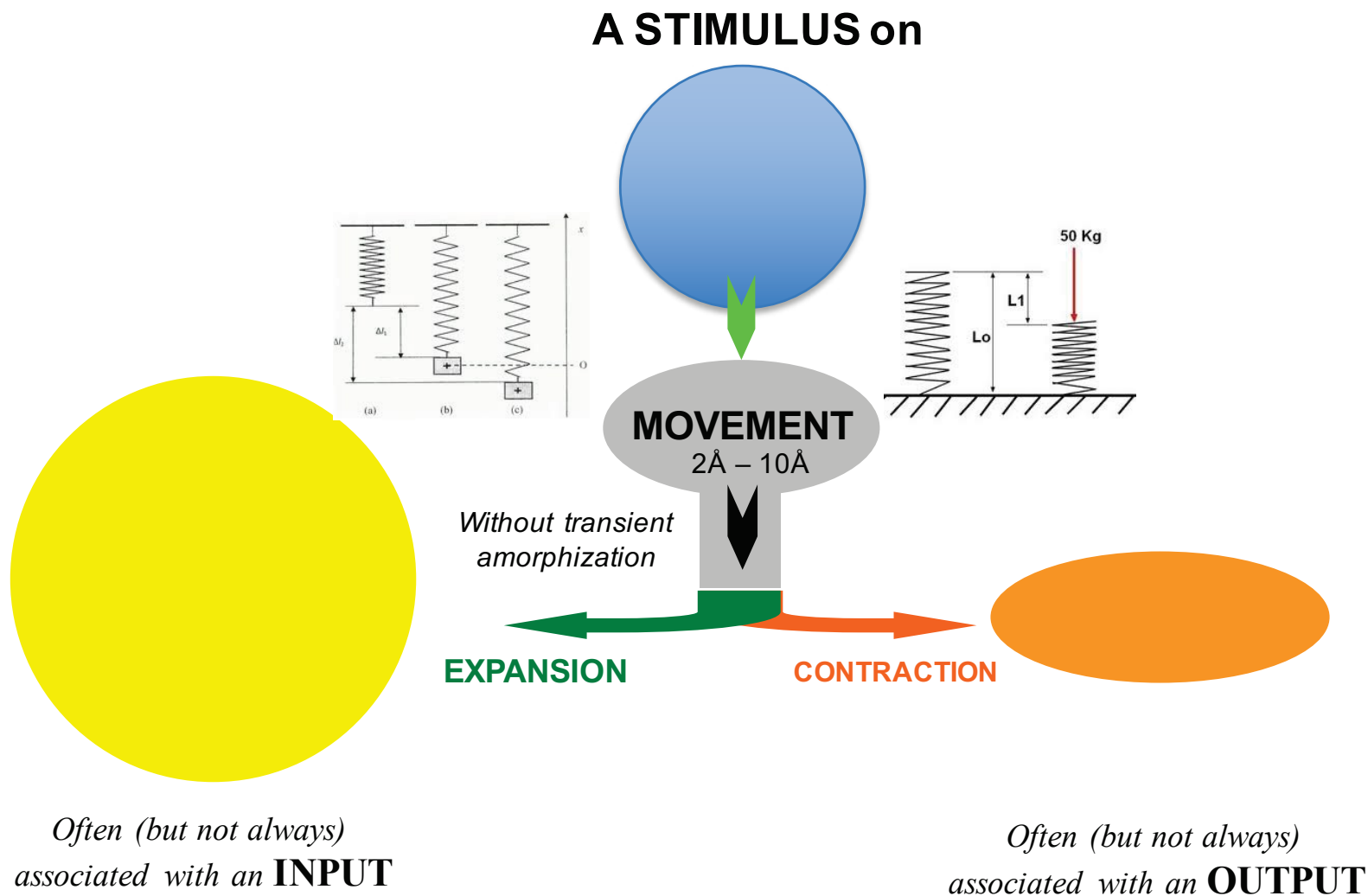


Fig.1. – Férey – Dalton issue



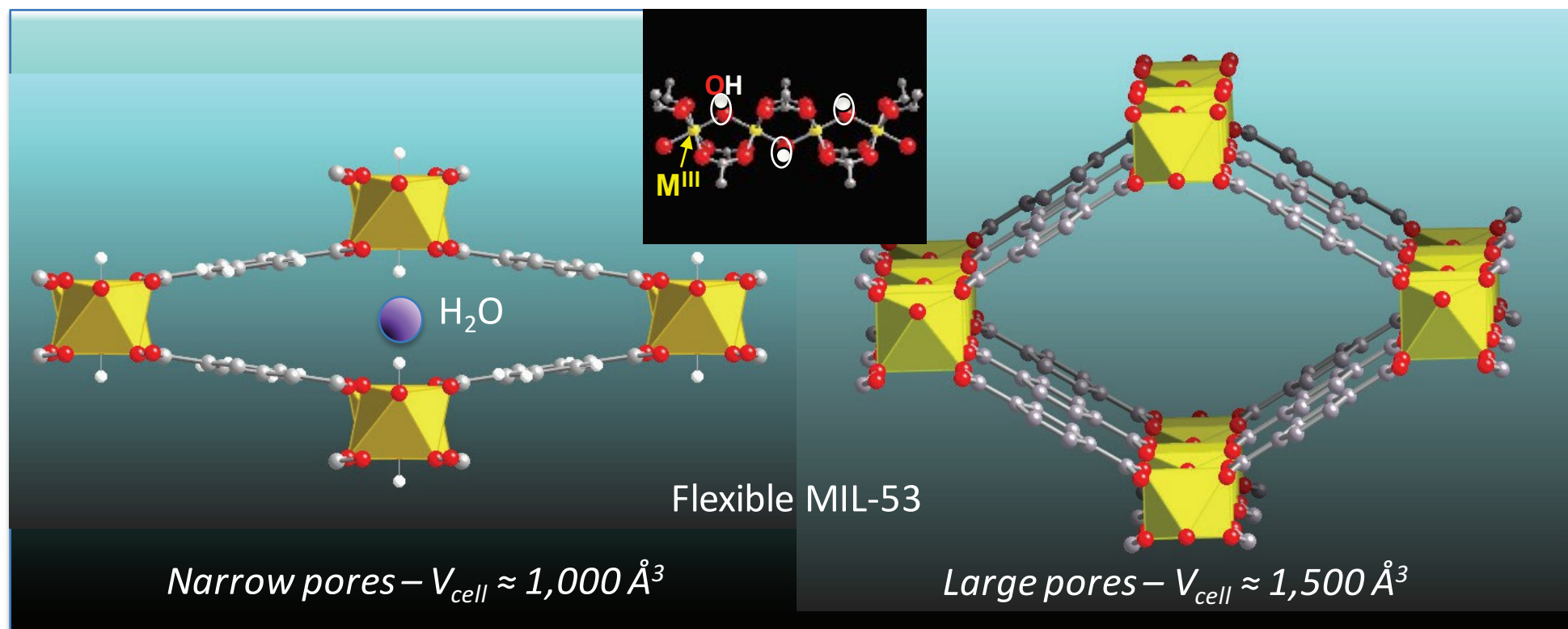


Fig.2. – Férey – Dalton issue

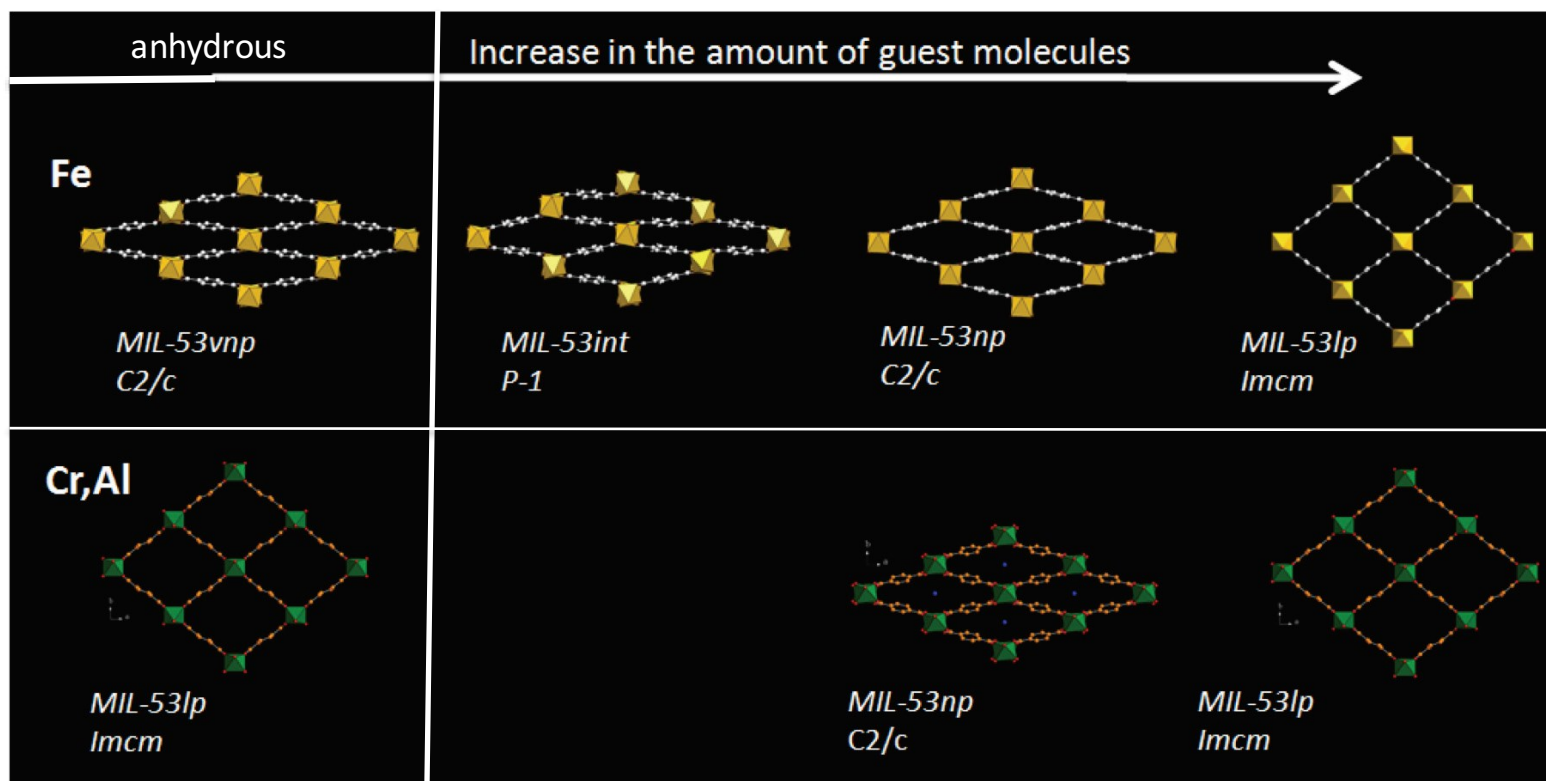


Fig.3. – Férey – Dalton issue

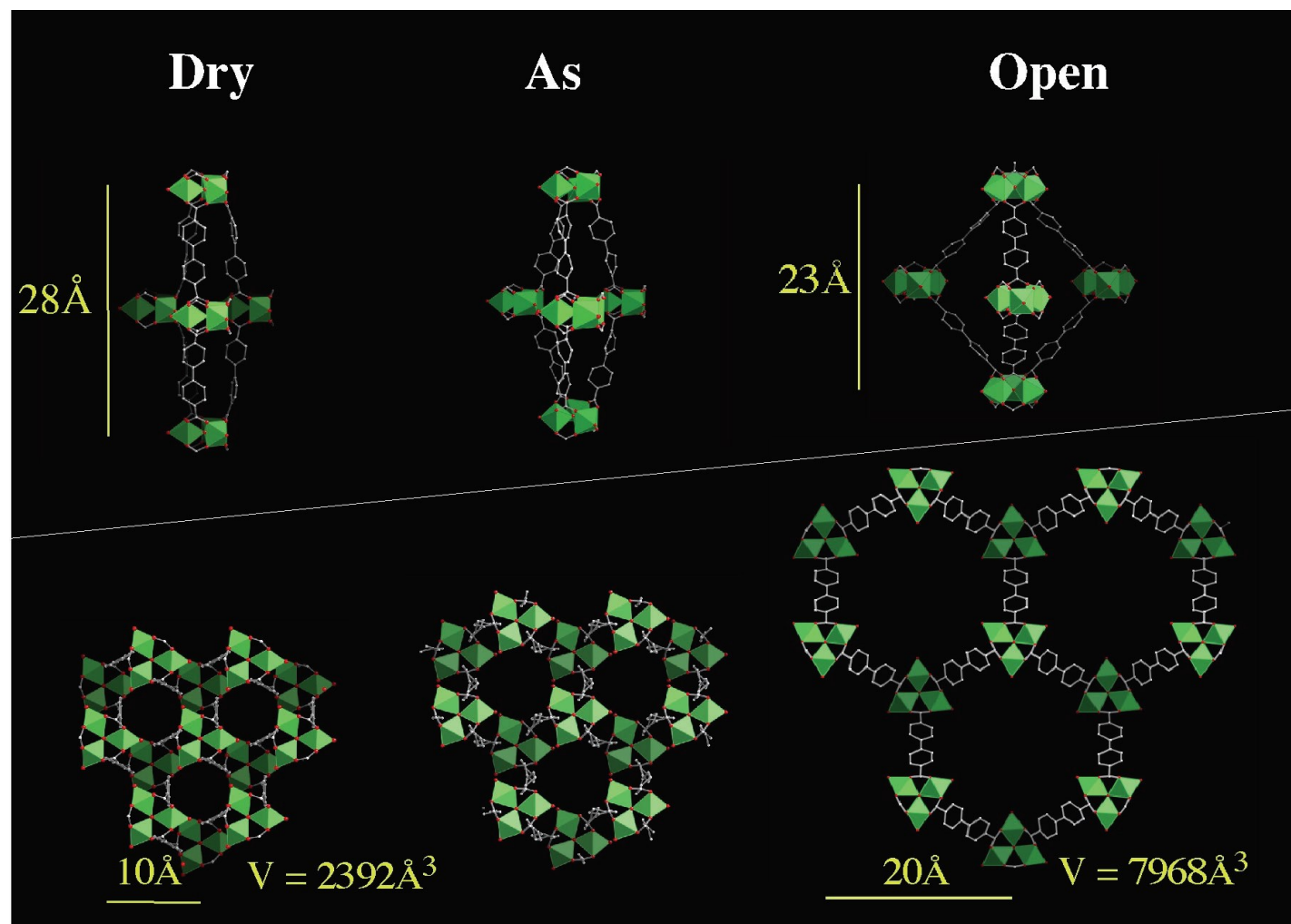


Fig.4. – Férey – Dalton issue

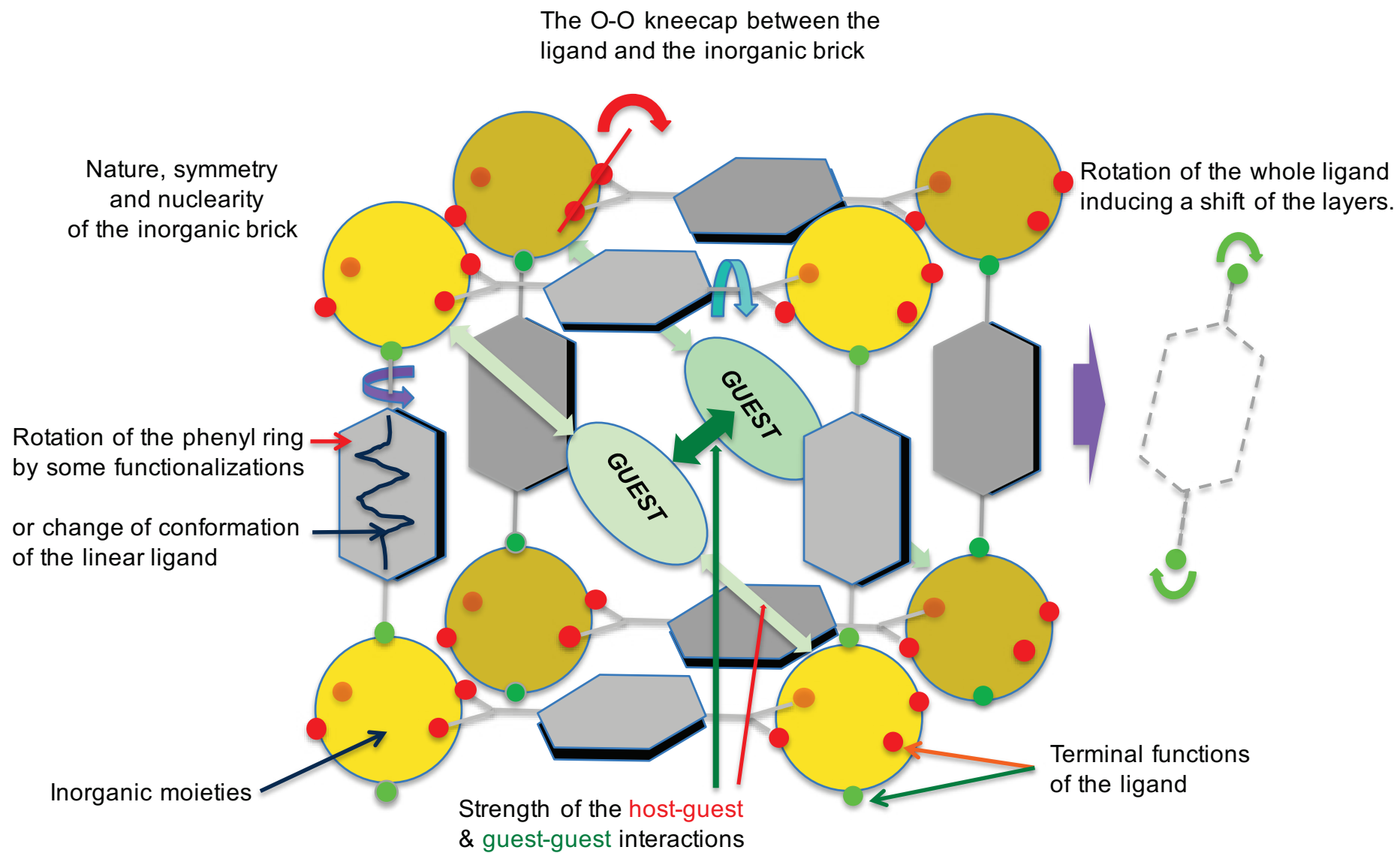


Fig.5. – Férey – Dalton issue

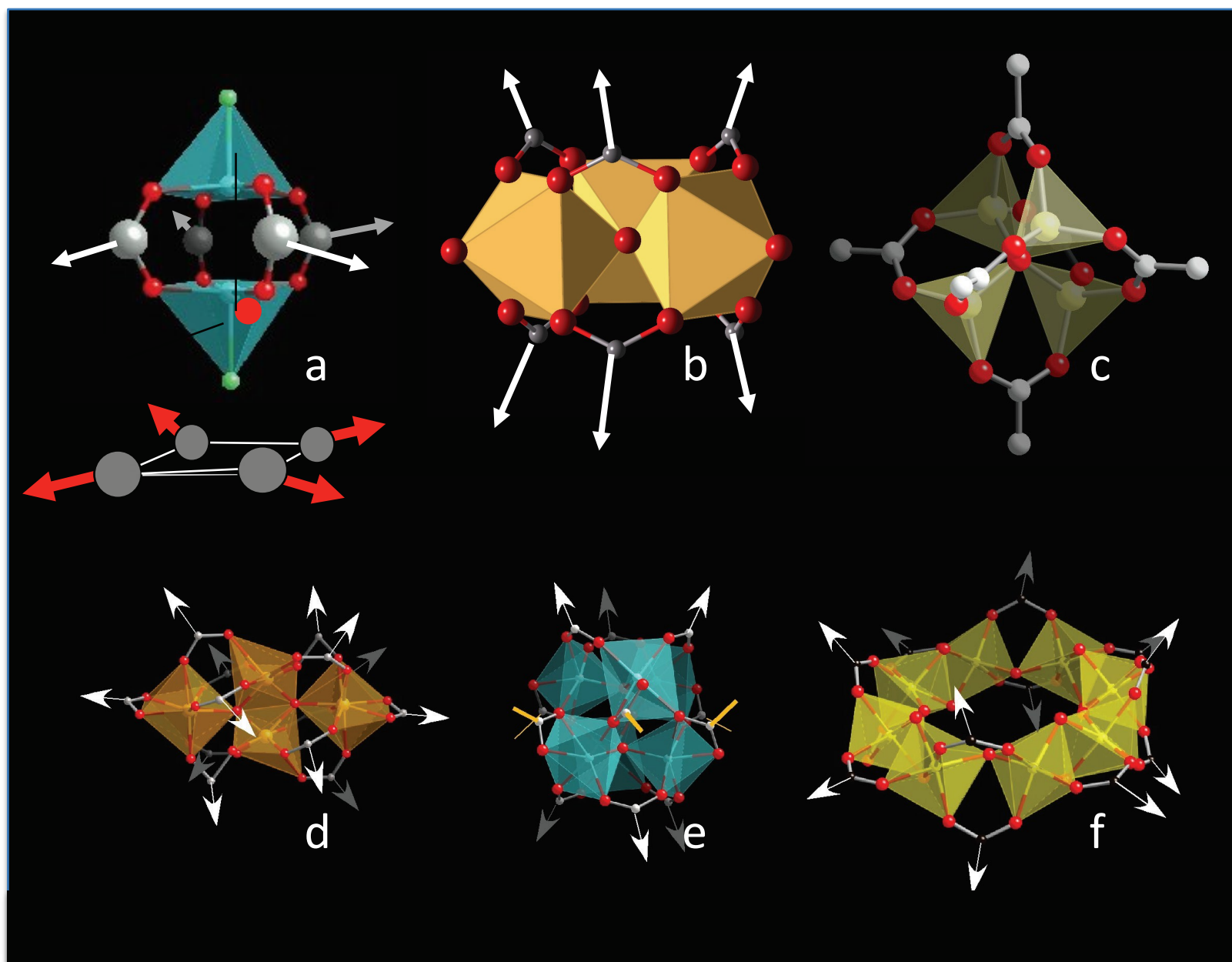


Fig.6. – Férey – Dalton issue

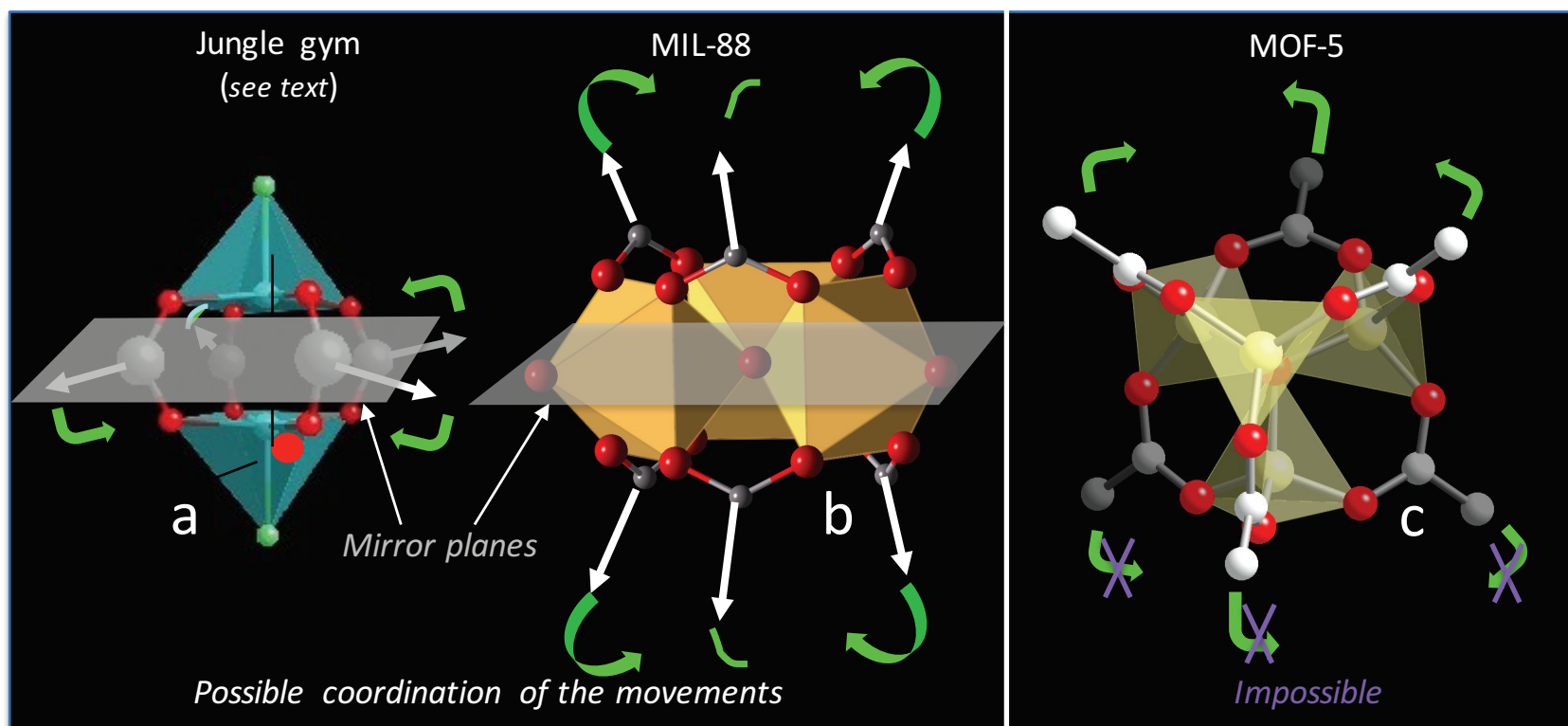


Fig.7. – Férey – Dalton issue

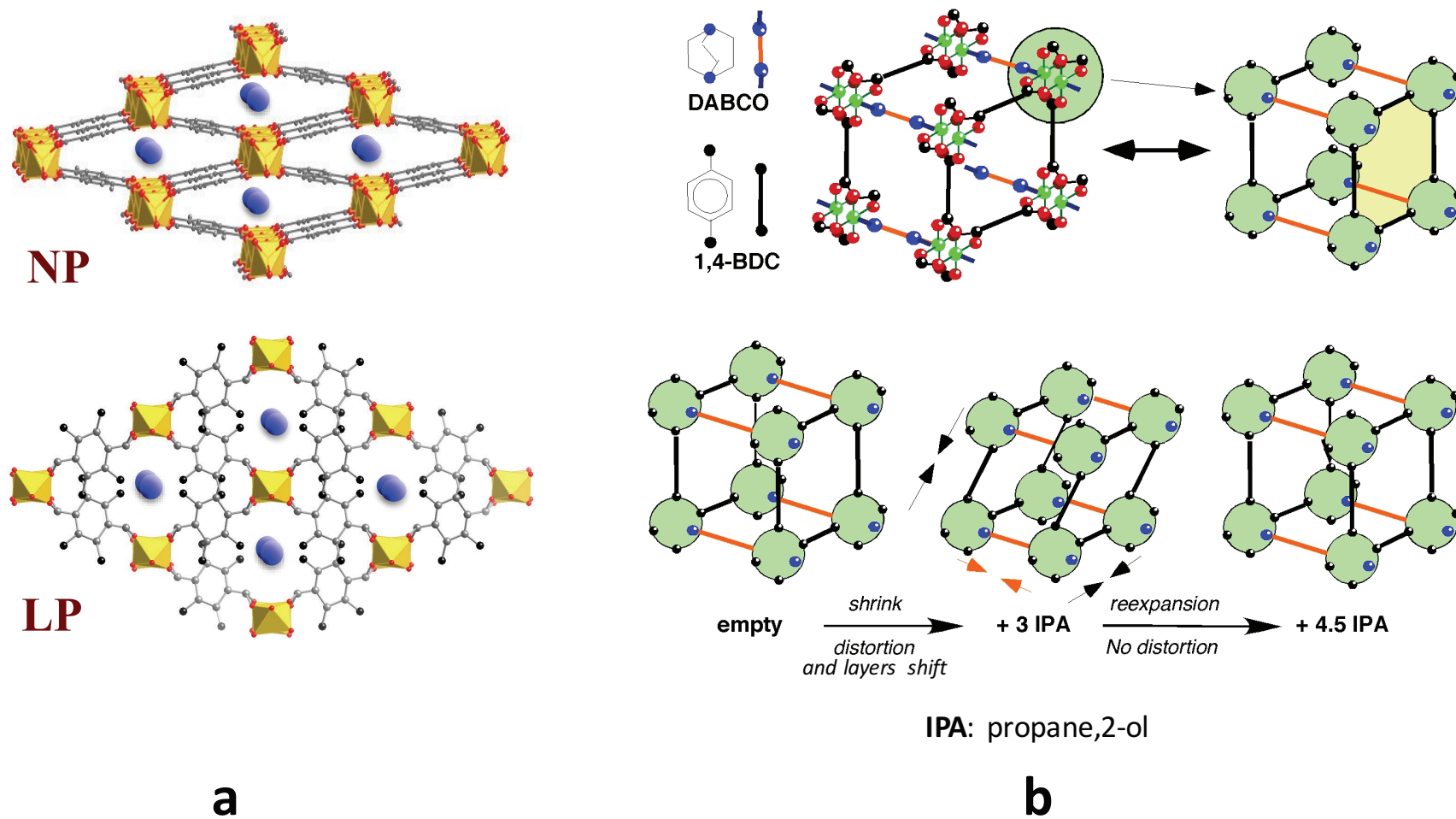


Fig.8. – Férey – Fajula issue NJC

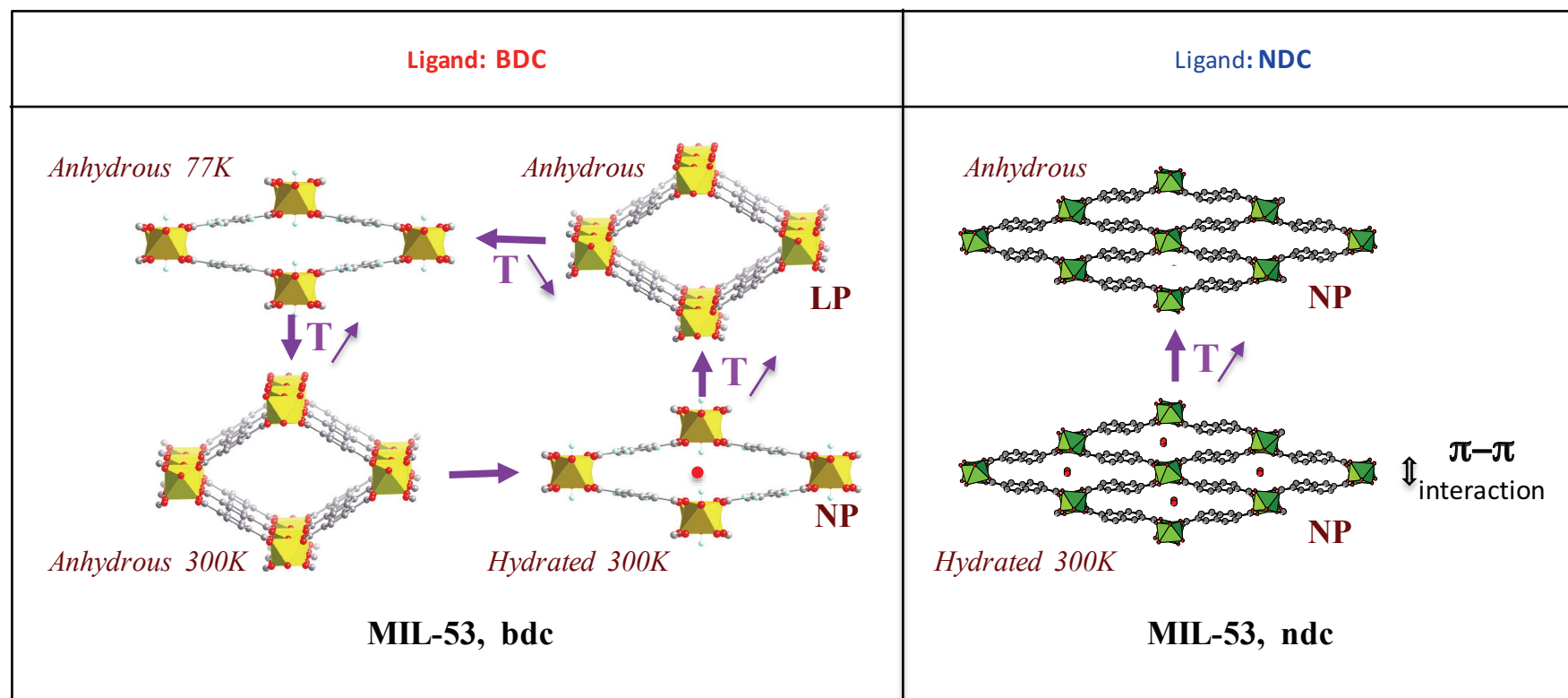


Fig 9. – Férey – Dalton issue



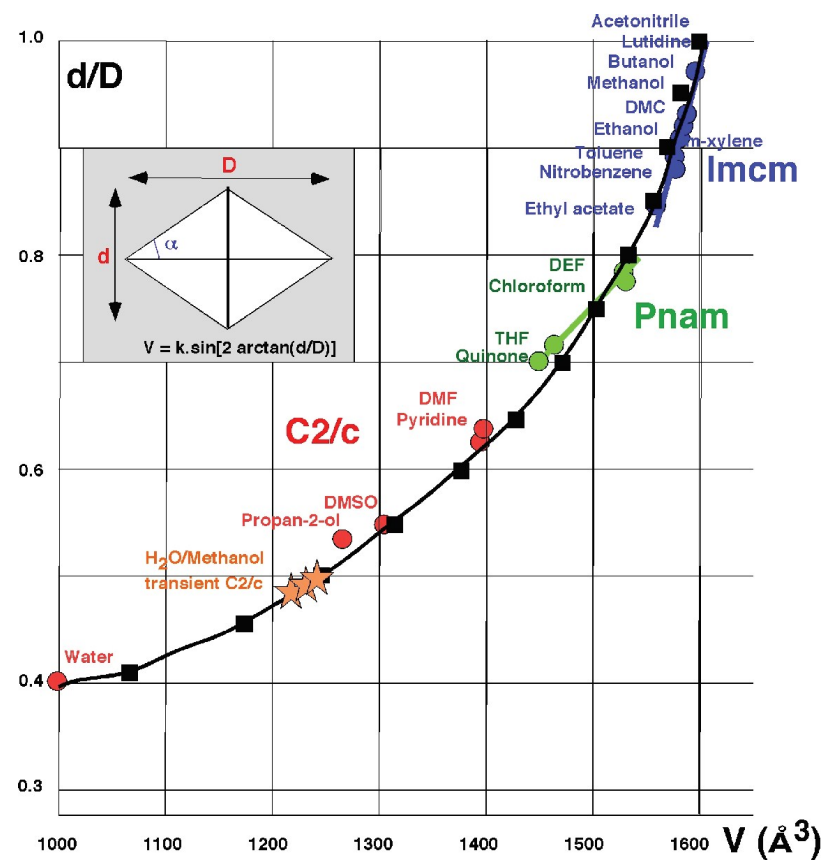
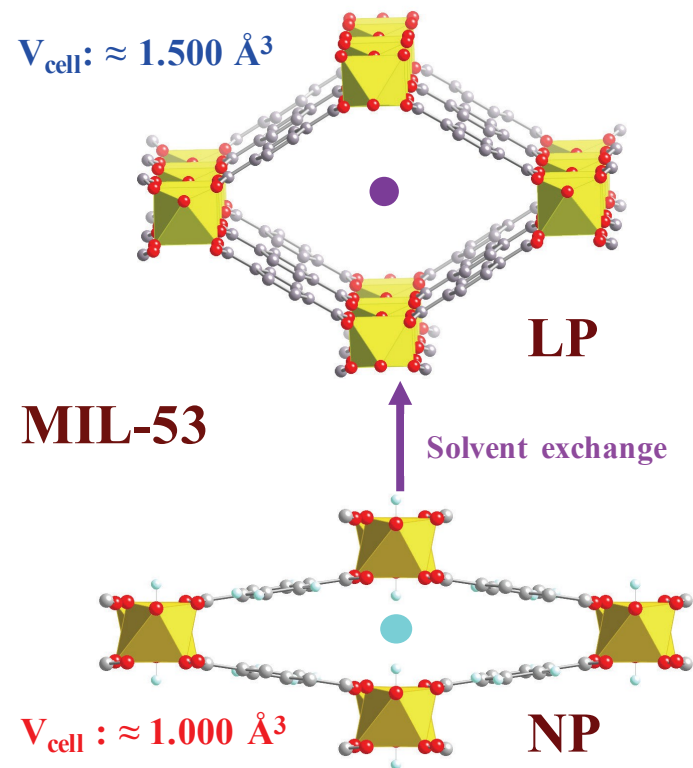


Fig 10. – Férey – Dalton issue

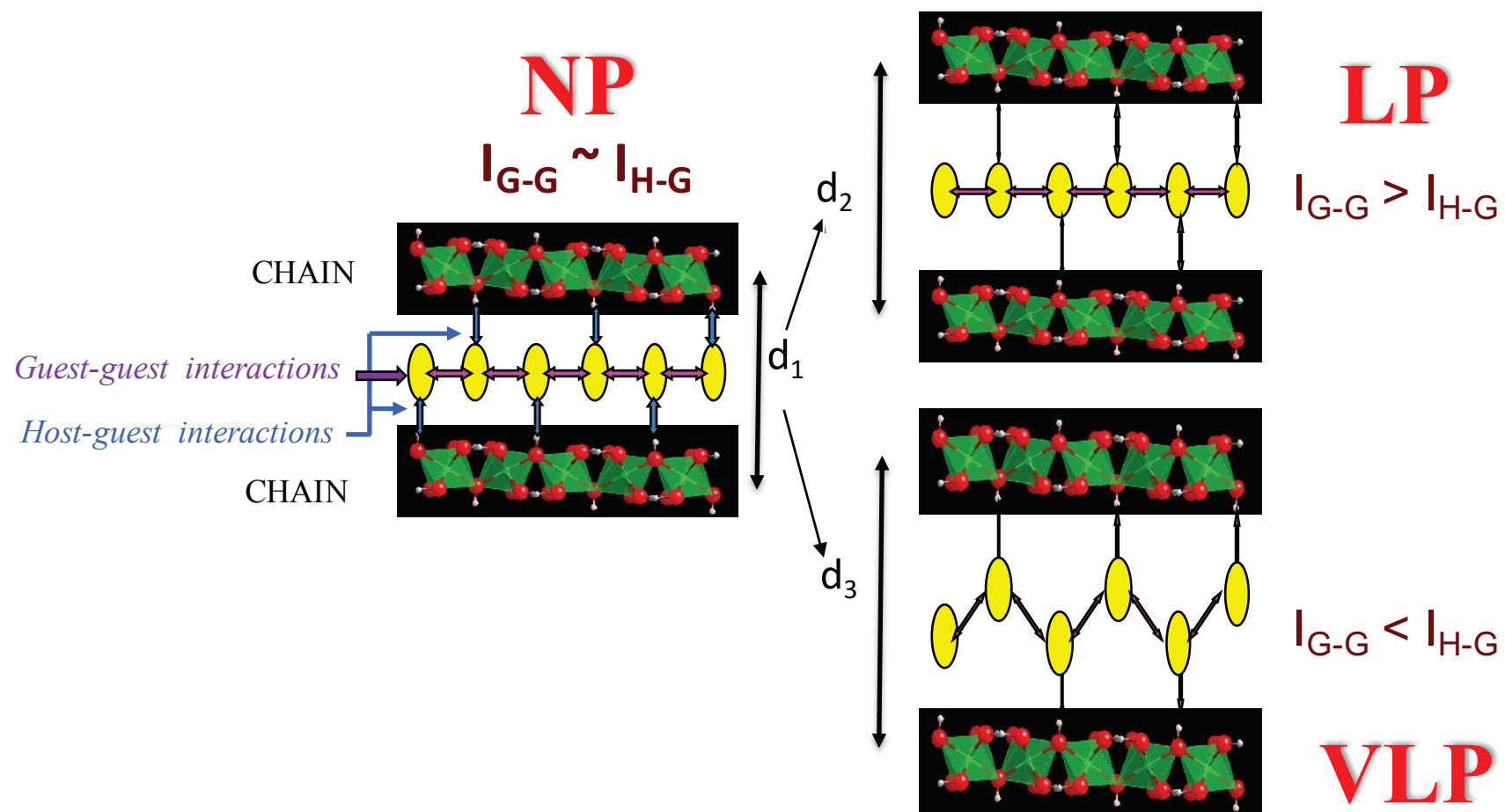


Fig 11. – Férey – Dalton issue

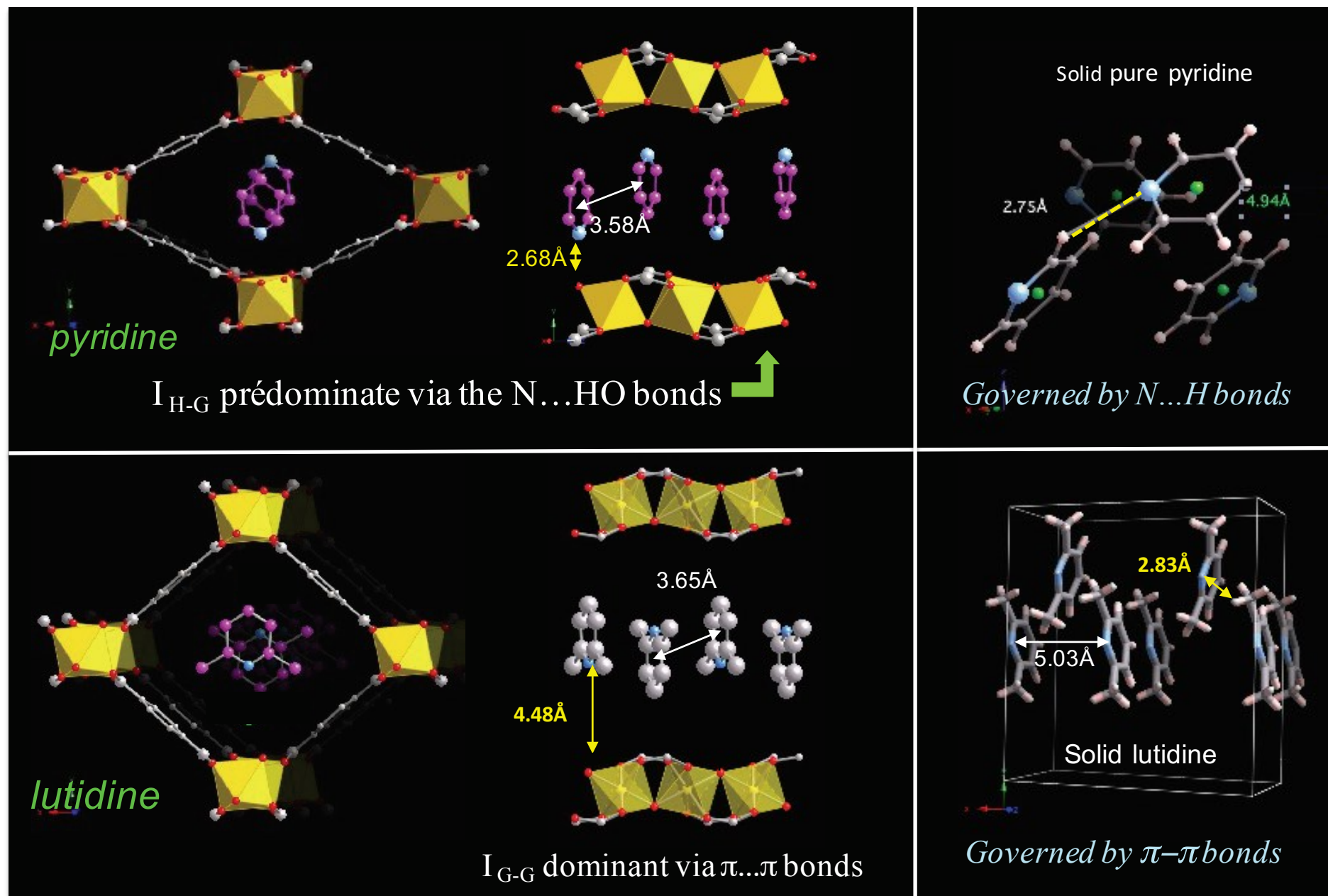


Fig 12. – Férey – Dalton issue

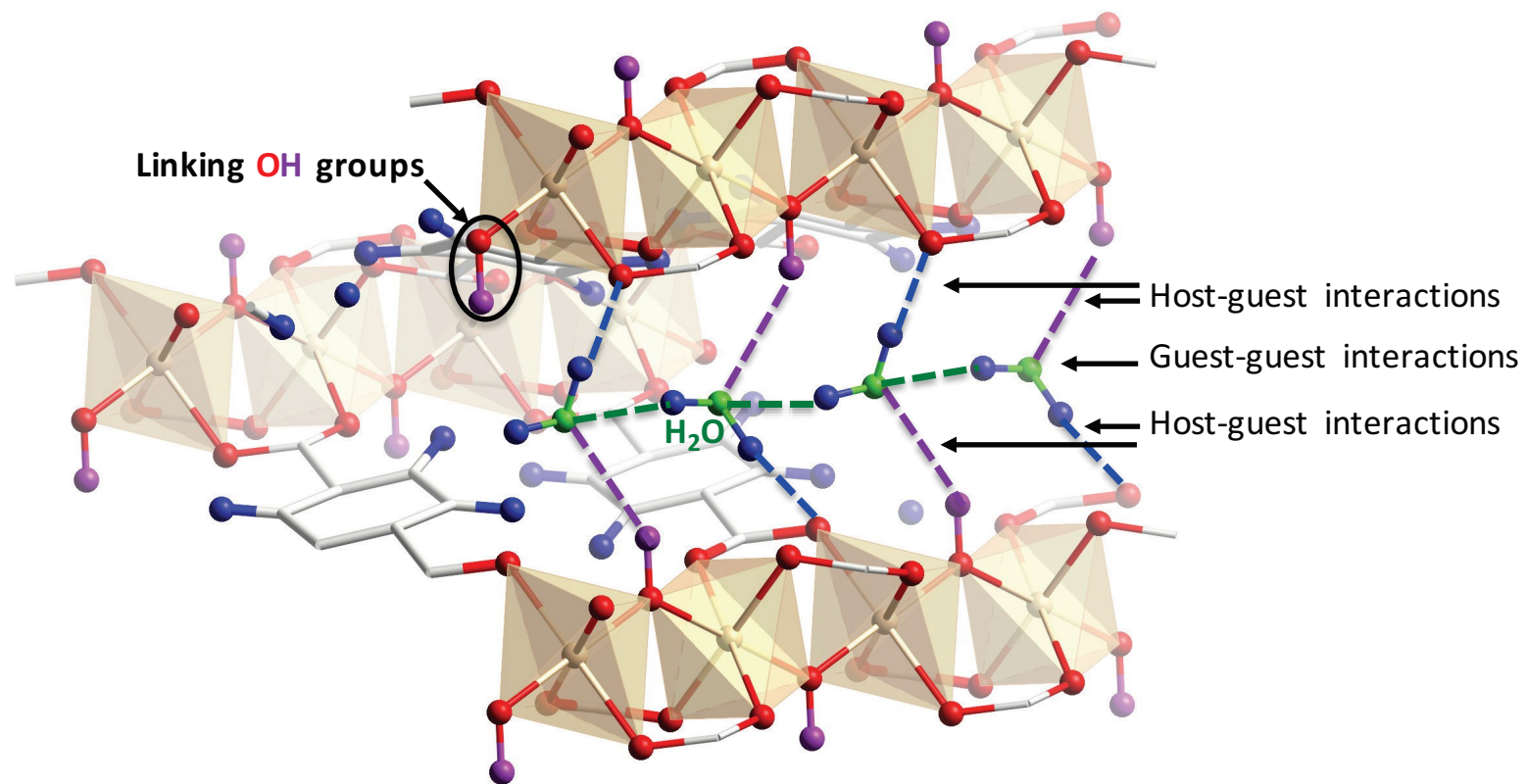
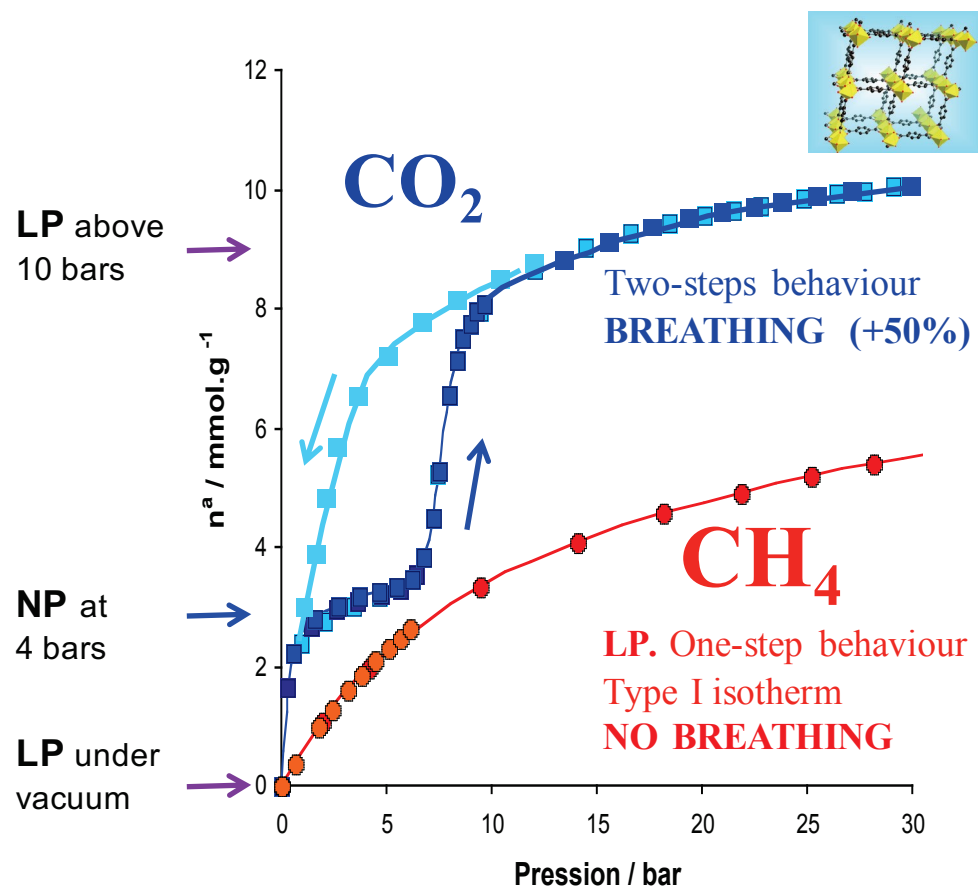
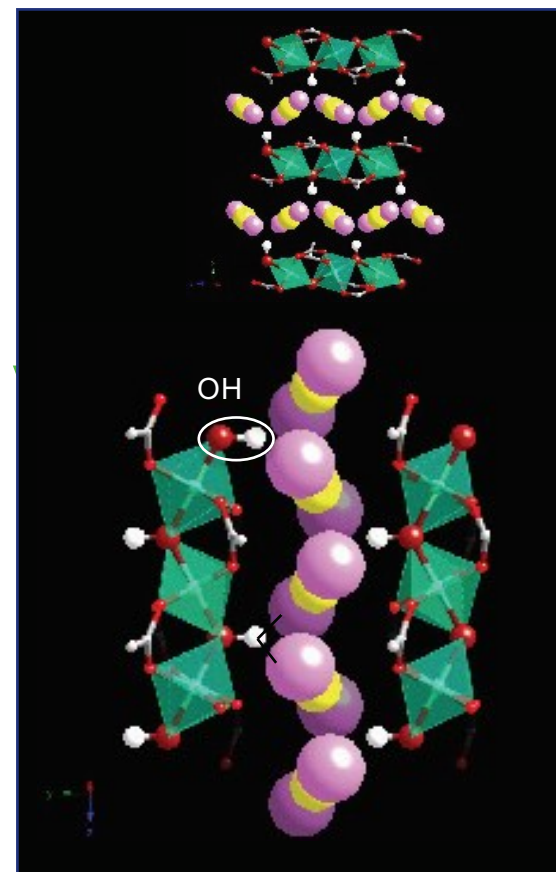


Fig 13. – Férey – Dalton issue



a



b

Fig 14. – Férey – Fajula issue NJC

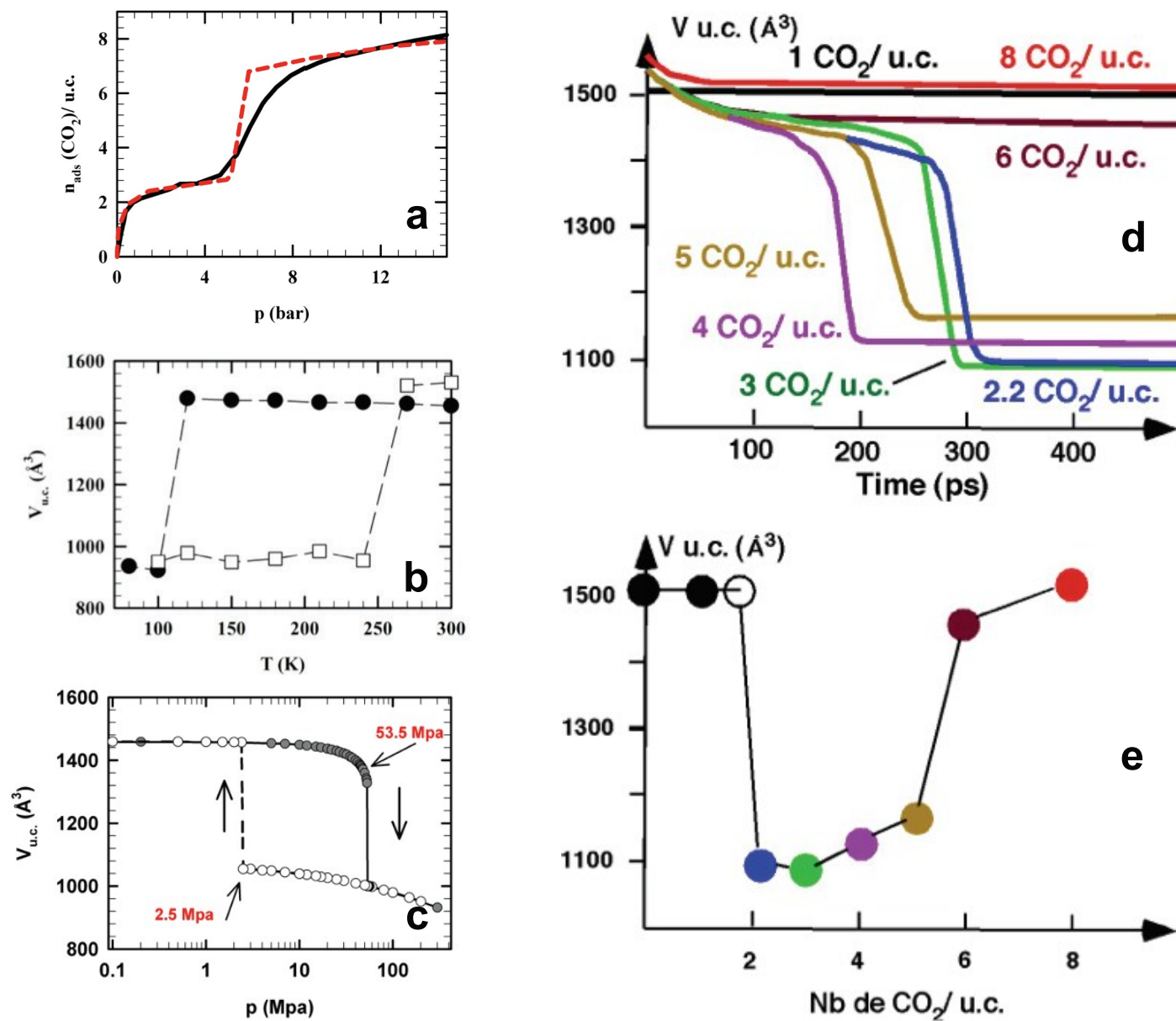


Fig 15. – Férey – Dalton issue

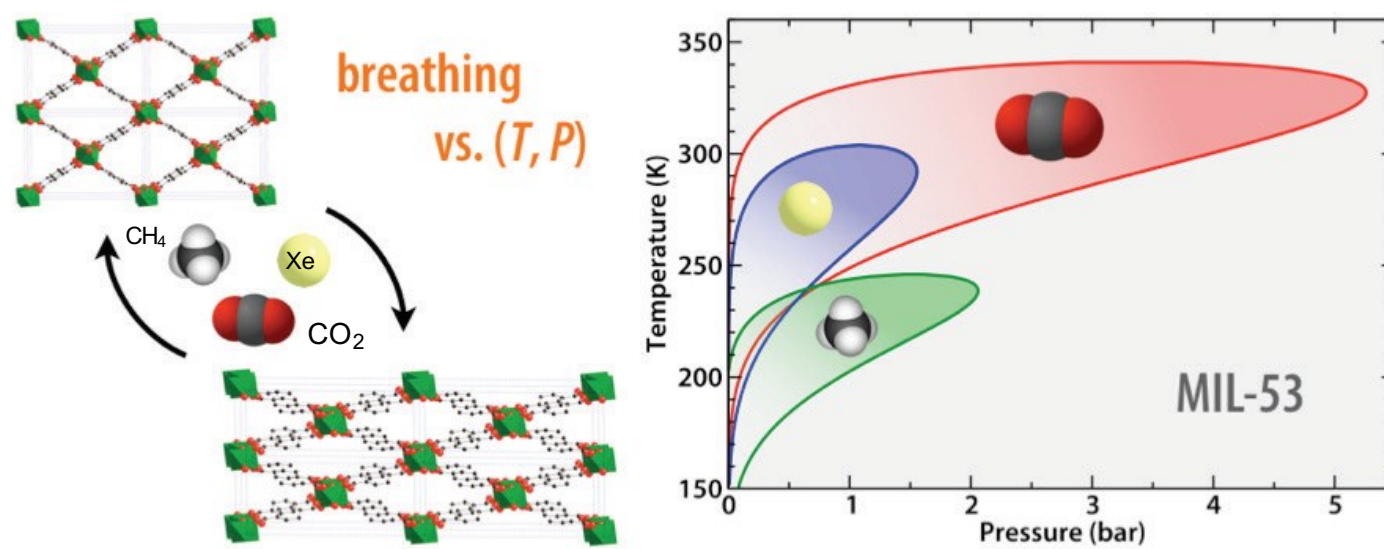
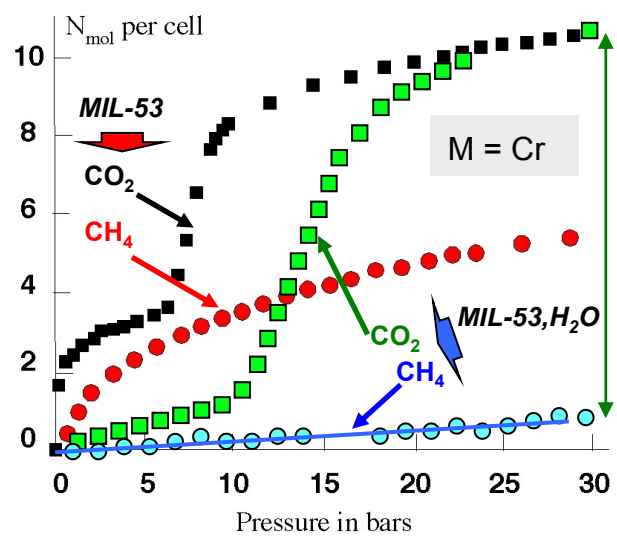
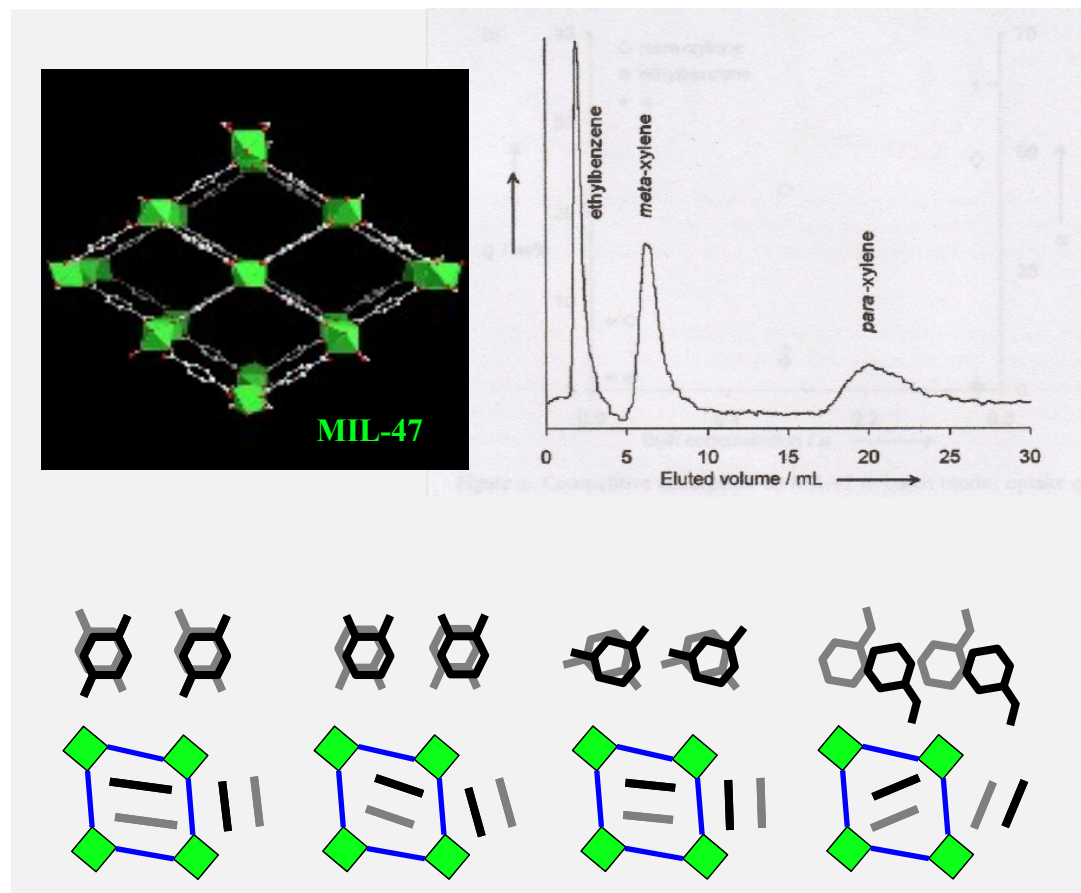


Fig 16. – Férey – Dalton issue



a



b

Fig 17. – Férey – Dalton



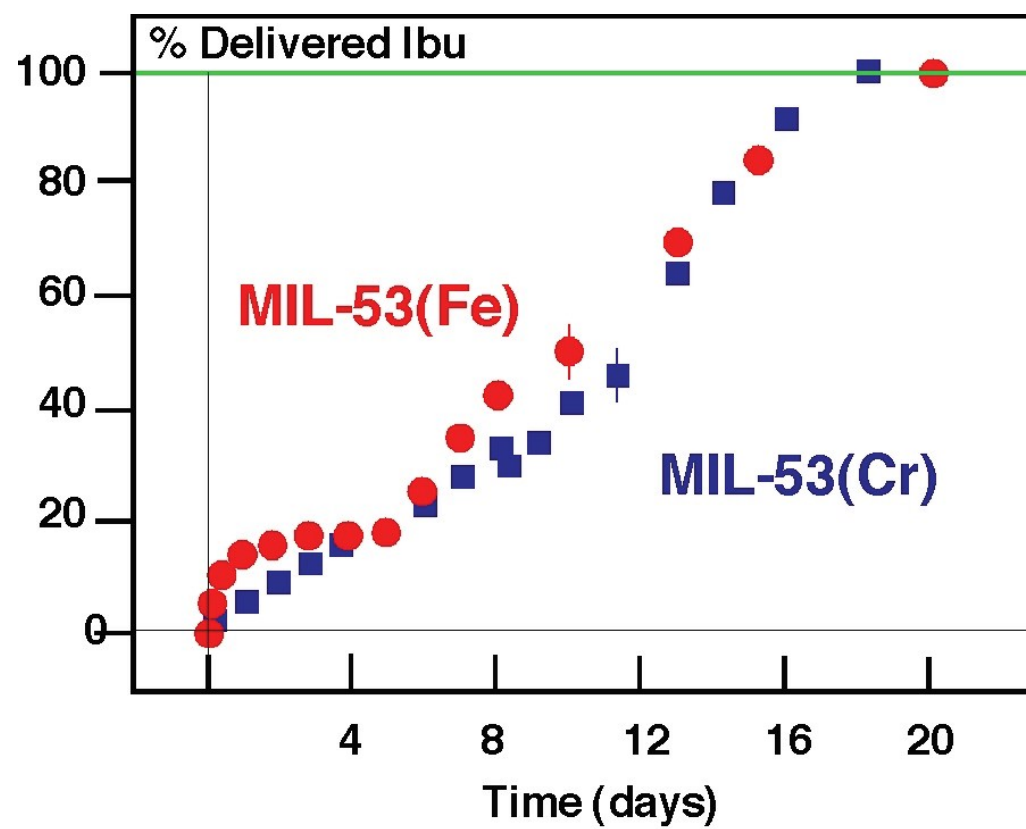


Fig 18. – Férey – Fajula issue NJC

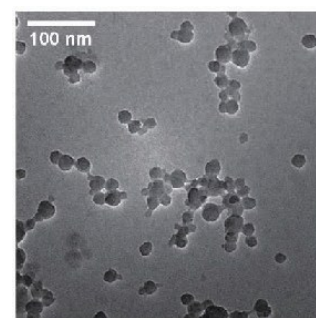
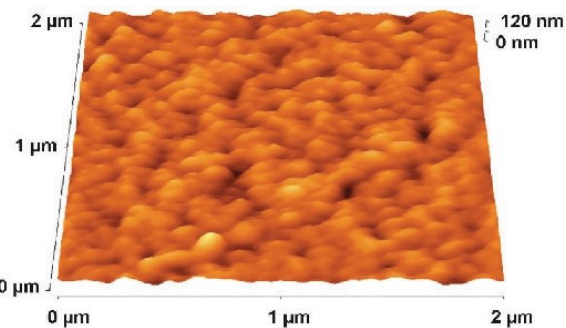
**a****c****d****e****b****f**

Fig 19. – Férey – Dalton issue